

Fengler, Matthias; Polivka, Jeanine

Conference Paper

Identifying Structural Shocks to Volatility through a Proxy-MGARCH Model

Beiträge zur Jahrestagung des Vereins für Socialpolitik 2022: Big Data in Economics

Provided in Cooperation with:

Verein für Socialpolitik / German Economic Association

Suggested Citation: Fengler, Matthias; Polivka, Jeanine (2022) : Identifying Structural Shocks to Volatility through a Proxy-MGARCH Model, Beiträge zur Jahrestagung des Vereins für Socialpolitik 2022: Big Data in Economics, ZBW - Leibniz Information Centre for Economics, Kiel, Hamburg

This Version is available at:

<https://hdl.handle.net/10419/264010>

Standard-Nutzungsbedingungen:

Die Dokumente auf EconStor dürfen zu eigenen wissenschaftlichen Zwecken und zum Privatgebrauch gespeichert und kopiert werden.

Sie dürfen die Dokumente nicht für öffentliche oder kommerzielle Zwecke vervielfältigen, öffentlich ausstellen, öffentlich zugänglich machen, vertreiben oder anderweitig nutzen.

Sofern die Verfasser die Dokumente unter Open-Content-Lizenzen (insbesondere CC-Lizenzen) zur Verfügung gestellt haben sollten, gelten abweichend von diesen Nutzungsbedingungen die in der dort genannten Lizenz gewährten Nutzungsrechte.

Terms of use:

Documents in EconStor may be saved and copied for your personal and scholarly purposes.

You are not to copy documents for public or commercial purposes, to exhibit the documents publicly, to make them publicly available on the internet, or to distribute or otherwise use the documents in public.

If the documents have been made available under an Open Content Licence (especially Creative Commons Licences), you may exercise further usage rights as specified in the indicated licence.

Identifying structural shocks to volatility through a proxy-MGARCH model*

Matthias Fengler[‡]

Jeannine Polivka[§]

Version: November 17, 2021

Abstract

We extend the classical MGARCH specification for volatility modeling by developing a structural multivariate GARCH (MGARCH) model targeting identification of shocks and volatility spillovers in a speculative return system. Similarly to the proxy-SVAR framework, we work with auxiliary proxy variables constructed from news-related measures to identify the underlying shock system. Our identification strategy targets full identification. We estimate the underlying structural rotation matrix by means of Givens rotations, which ensures orthogonality of the resulting shocks. In an empirical application, we identify an equity, bond and currency shock. We study the volatility spillovers implied by these labeled structural shocks. Our analysis shows that symmetric spillover regimes are rejected.

Keywords: Givens rotations, identification, news-based measures, proxy-MGARCH, shock labelling, structural innovations, volatility spillovers

JEL: C32, C51, C58, G12

*We are grateful for financial support by the Swiss National Science Foundation (SNF Grant No: 176684, Project “Structural Models of Volatility”). For constructive comments on previous versions of this article, the authors thank the conference participants of the NBER-NSF Time Series Conference, SoFiE, the 14th Annual Risk Management Conference of NUS RMI and the Conference of the Swiss Society of Economics and Statistics (SSES) 2021 and the research seminar participants of TU Dresden, University of Sussex, UCL and University of Bologna, in particular Luca Fanelli.

[‡]School of Economics and Political Science, Department of Economics, University of St. Gallen, Bodanstrasse 6, 9000 St. Gallen, Switzerland. Email: matthias.fengler@unisg.ch.

[§]School of Economics and Political Science, Department of Economics, University of St. Gallen, Bodanstrasse 6, 9000 St. Gallen, Switzerland. Email: jeannine.polivka@unisg.ch.

1 Introduction

A primary objective of multivariate volatility models is accurately describing the stylized facts of asset returns and their second-order moment dynamics. Much effort has therefore been devoted to precisely capturing the salient features of financial returns, such as fat tails, leverage effects and time-varying cross-asset dependencies (Andersen et al., 2009; Bauwens et al., 2012). While their widespread use is a vivid testimony to their success, extant multivariate volatility models do little in terms of offering an intelligible interpretation of the shock system which drives asset returns: they are merely reduced form models. This stands in sharp contrast to macroeconomics which has seen the development of structural models alongside reduced form models (Taylor and Uhlig, 2016). Besides reflecting the pertinent features of the modeled economic system, structural models at the same time identify the shock system. As a key advantage, they allow for counterfactual policy and business cycle analysis and an economic interpretation of shocks. In the extant literature on multivariate volatility models such a modeling framework is currently missing.

In this work, we make a first step towards extending reduced form multivariate volatility models of the GARCH form (MGARCH) to structural models in the macroeconometric sense. We achieve this goal by estimating a time-invariant rotation matrix, which transforms the vector of uncorrelated structural shocks into a correlated mixture of standardized reduced-form errors. The latter are subsequently multiplied with the principal matrix square root of the the time-varying covariance matrix and drive the speculative asset return system. The approach identifies the structural shocks because in the MGARCH model the multivariate variance process is fully identified and the estimation of the rotation matrix occurs conditionally on the initial choice of the matrix square root of the covariance matrix process. Thus, the set of structural parameters of interest are not the

dynamic model parameters but the rotation matrix.

Necessarily, the estimation of the structural rotation requires identifying restrictions. While in the macroeconometric literature economic theory has furnished a valuable resource for identifying assumptions, it offers little guidance on establishing identifying restrictions in high-frequency speculative asset return systems. Indeed, the interconnectedness and fast-paced nature of financial markets seem to rule out the classical repertoire of identifying restrictions used in the macroeconomic SVAR literature (see [Amisano and Giannini \(1997\)](#) and [Kilian and Lütkepohl \(2017\)](#) for overviews) such as short- and long-run restrictions, sign restrictions and exclusion or ordering restrictions imposed on the reduced form model.

For this reason, we follow ideas developed in the narrative identification approach of [Romer and Romer \(2010\)](#) and [Mertens and Ravn \(2013\)](#) and [Stock and Watson \(2012, 2016, 2018\)](#) and exploit information ingrained in external fundamental data to identify our shocks. As regards multivariate volatility models, we argue that the increasing availability of narrative records and news data at high frequency offers an untapped potential for proxy-based identification of reduced form volatility models. Our identification strategy allows for full identification of the rotation angles of the structural rotation by means of a general recurrence scheme using Givens rotations, which ensures orthogonality of the identified shocks. As a result, we obtain a structural decomposition of the multivariate volatility system and labeled structural shocks.

Using news data for identification in volatility models appears to be very natural given the notion of a link between information flows and volatility has been present in volatility modeling since its beginnings: consider the mixture of distributions hypothesis of [Clark \(1973\)](#), the news impact curve ([Engle and Ng, 1993](#)) and the reaction of financial markets

to information at high frequency (Groß-Klußmann and Hautsch, 2011; Bollerslev et al., 2018; Boudoukh et al., 2018). Our identification strategy builds on the understanding that news items can represent public fundamental information which drives returns and volatility when prices respond to it.

Naturally, we are not the first to address identification in model specifications with heteroscedasticity. The class of VAR models with stochastic volatility initially suggested by Primiceri (2005) is however barely attractive for standard applications in empirical finance because daily return series typically feature large time dimensions and their (co-)variances are assumed to be stationary. Moreover, heteroscedastic SVARs commonly deal with a different identification problem. For example, the identification by heteroscedasticity approach pioneered by Rigobon (2003) and further explored by Lanne et al. (2010), Weber (2010) and Lütkepohl and Schlaak (2021) assumes (conditionally) heteroscedastic structural shocks to infer a structural representation focusing on the dynamics of the mean equation with constant impact effects of structural shocks. In contrast, our identification approach acknowledges that for the purpose of asset return modeling, it is desirable to allow for complex dynamics in the covariance generating mechanisms of the reduced form innovations. By modeling the conditional covariance process of the reduced form errors by an MGARCH model while assuming white noise structural shocks, we permit such flexibility. The identification problem in this context consists of finding a structural decomposition of the conditional covariance process to recover the structural shocks driving the multivariate volatility model. Hafner et al. (2020) tackle this in the tradition of independent component analysis which exploits the fact that under independence of the structural components at most one component can be Gaussian. However, statistical identification approaches do not necessarily deliver structural shocks which are economically meaningful. In contrast, our identification scheme delivers readily interpretable labeled shocks.

In our empirical application, we study a system of speculative asset returns of core interest to the U.S. economy: the S&P 500, the yield of the U.S. constant maturity 10 year treasury note and a USD index basket. As proxy variables, we use the Thomson Reuters news sentiment indicators of the U.S. stock and the U.S. bond market which allows us to uncover a fully identified asset return system, driven by an equity shock, a bond shock and a currency shock. To further corroborate these labels, we make the additional effort to trace the most extreme shock observations back to major financial and economic events. We find evidence that the volatility spillovers are clearly non-symmetric, which invalidates spectral decompositions, and change considerably over time and with the local and global economic state. For example, we discover that the share of impact of the equity shock on the S&P 500 returns has diminished from 1998 to 2012 – a trend starting long before the financial crisis of 2008 – with impact shifting to the treasury yield returns instead. This finding complements a strand of literature investigating the link between fixed income and equity markets (Rigobon and Sack, 2003; Ehrmann et al., 2011).

The remainder of the paper is structured as follows. In Section 2, we present the structural identification strategy using proxy variables. Section 3 lays out the MGARCH estimation underlying the identification. The results of the empirical application of our model are provided in Section 4. Section 5 concludes.

2 Structural identification

2.1 Rotation invariance and identification problem

We consider the system of n speculative (log) returns given by

$$r_t = \mu + \varepsilon_t \quad (t \in I := \{1, \dots, T\}) \quad (1)$$

where we set $\mu = 0$, as our focus is on volatility spillovers rather than mean dynamics. The n -dimensional reduced-form innovation vector ε_t satisfies

$$\begin{aligned} \mathbb{E}[\varepsilon_t | \mathcal{F}_{t-1}] &= 0 \\ \mathbb{E}[\varepsilon_t \varepsilon_t^\top | \mathcal{F}_{t-1}] &= H_t, \end{aligned} \quad (2)$$

where \mathcal{F}_t is the σ -algebra generated by the returns up to and including time t . The conditional covariance matrix H_t is assumed to be positive definite and symmetric with probability one and can be allowed to display any MGARCH or DCC type dynamics. The statistical innovations ε_t do not bear an economic interpretation. To endow the model with a structural meaning, let ε_t be generated according to

$$\varepsilon_t | \mathcal{F}_{t-1} \sim Q_t \xi_t, \quad (3)$$

where $(\xi_t)_{t \in I}$ is an n -dimensional vector of structural shocks with $\mathbb{E}[\xi_t] = 0$ and $\mathbb{E}[\xi_t \xi_t^\top] = I_n$, the n -dimensional identity matrix. Q_t denotes an a priori unknown structural matrix decomposition of H_t which satisfies $Q_t Q_t^\top = H_t$. It is the transmission mechanism of the underlying economy that translates the structural shock ξ_t into the observable reduced-form innovation ε_t . For identification we assume that Q_t is positive definite.¹ It is well-known that this decomposition is unique up to an orthogonal transformation (Horn and Johnson, 2012, Theorem 7.3.11). Thus, if we can identify this transformation, we can determine the structural matrix decomposition underlying the asset return system, even

¹By $(-Q_t)(-Q_t)^\top = H_t$, Q_t could be taken to be negative definite, too.

when Q_t is time-varying. We assume that this particular matrix decomposition is time-invariant.

To see the identification problem more clearly, let \tilde{Q}_t be any matrix decomposition such that $H_t = \tilde{Q}_t \tilde{Q}_t^\top$. One obtains another observationally equivalent decomposition by setting

$$H_t = \tilde{Q}_t \tilde{Q}_t^\top = \tilde{Q}_t R R^\top \tilde{Q}_t^\top = (\tilde{Q}_t R) (\tilde{Q}_t R)^\top, \quad (4)$$

where R is a real ($n \times n$) rotation matrix satisfying

$$\begin{aligned} R^\top R = R R^\top &= I_n && \text{(orthogonality)} \\ \det(R) &= +1 && \text{(proper rotation)}. \end{aligned} \quad (5)$$

Given an initial decomposition \tilde{Q}_t , identification of the true structural matrix decomposition Q_t thus amounts to identifying the unique rotation \tilde{R} such that $\tilde{Q}_t \tilde{R} = Q_t$. The structural model parameters are thus given by the elements of the rotation matrix, respectively by the angles defining the rotation. Formulating identification problems in terms of rotations has become increasingly popular in recent years, especially in Bayesian frameworks (Giacomini et al., 2021; Arias et al., 2021) but also in frequentist models (Fisher and Huh, 2019) and the statistically identified MGARCH model of Hafner et al. (2020).

Because of non-identification, the choice of the matrix decomposition is often determined by an ad-hoc decision. For instance, popular choices are the principal square root, which is obtained from an eigenvalue decomposition of H_t , or the Cholesky factorization of H_t . While symmetric volatility spillovers as imposed through eigenvalue decompositions are undoubtedly a strong assumption for financial return data, assuming a causal chain structure in economic shocks to daily speculative returns through a Cholesky decomposition may only be debatable for certain special asset systems and requires cogent economic justification. For this reason, we suggest employing additional external information about the economy to properly identify the structural rotation.

It is important to note that this identification problem differs from the one in the SVAR case. When coupling economic identification with modeled heteroscedasticity, the SVAR literature models structural shocks w_t by $w_t = B\epsilon_t$ and assumes w_t to be heteroscedastic such that $E[\epsilon_t\epsilon_t^\top] = B^{-1}\Lambda_t B^{-1\top}$ where Λ_t is the time-varying diagonal variance matrix of the structural shocks (Lütkepohl and Schlaak, 2021). It is clear that for the purpose of asset return modeling this assumption is restrictive as it does not allow one to retain the complex dynamics of the covariance generating process. Therefore the identification problem we are handling in the MGARCH case treats heteroscedastic reduced form innovations (returns) based on homoscedastic structural shocks.

2.2 Identification by proxy

Because the true structural relationship in (3) is unobserved, we consider the principal matrix square root \tilde{Q}_t as initial decomposition of H_t . The reason is that the principal square root is known to be positive definite if and only if H_t is² and positive definiteness of \tilde{Q}_t ensures invertibility of all other matrix decompositions $\tilde{Q}_t R$: Indeed, the existence of an $(n \times n)$ matrix \tilde{Q}_t^{-1} such that $\tilde{Q}_t^{-1}\tilde{Q}_t = I_n$ implies that, for any $(n \times n)$ rotation matrix R , there exists a matrix $B = (\tilde{Q}_t R)^{-1}$ such that $B(\tilde{Q}_t R) = R^{-1}\tilde{Q}_t^{-1}\tilde{Q}_t R = I_n$ because $\det(R) = +1$.

²A real symmetric $(n \times n)$ matrix H can be factorized as $H = \Gamma\Lambda\Gamma^\top$; here, Γ is an orthogonal $(n \times n)$ matrix, with the normalized eigenvectors of H as columns, and Λ is a diagonal matrix of the eigenvalues. The principal square root of H is defined as $\Gamma\Lambda^{1/2}\Gamma^\top$ where $\Lambda^{1/2}$ denotes the diagonal matrix of the square root of the eigenvalues. It is the unique square root which has non-negative eigenvalues see Horn and Johnson (2012, Theorem 7.2.6).

Given that H_t is \mathcal{F}_{t-1} -measurable, we define standardized residuals u_t by

$$\begin{aligned} \varepsilon_t &= Q_t \xi_t = \tilde{Q}_t \tilde{R} \xi_t \\ \Leftrightarrow \tilde{R} \xi_t &= (\tilde{Q}_t)^{-1} \varepsilon_t =: u_t \end{aligned} \quad (6)$$

We decompose the $(n \times n)$ matrix \tilde{R} into the vector $\tilde{R}_{\cdot 1}$ corresponding to the first column of \tilde{R} and an $((n \times (n - 1)))$ remainder matrix \tilde{R}^* . Correspondingly, we split ξ_t into a shock of interest ξ_{1t} , which, without loss of generality, can be assumed to be the first vector entry, and a remainder ξ_t^{1*} . This decomposition yields:

$$u_t = \tilde{R}_{\cdot 1} \xi_{1t} + \tilde{R}^* \xi_t^{1*} \quad (7)$$

Hence, for partial identification of the model, we need an estimate of $\tilde{R}_{\cdot 1}$.

In many cases however, one is interested in full identification of the underlying structural model, i.e. an estimate of \tilde{R} . To this end, we build on ideas of [Stock and Watson \(2012\)](#) and [Mertens and Ravn \(2013\)](#). Assume there exists a centered $(n - 1)$ -dimensional instrument process $Z = (Z_t)_{t \in I}$ such that, for all $i = 1, \dots, n - 1$,

$$E[\xi_{it} Z_{it}] = \phi_i \in \mathbb{R} \setminus \{0\} \quad (\text{relevance}) \quad (8)$$

$$E[\xi_t^{i*} Z_{it}] = \mathbf{0}_{(n-1) \times 1} \quad (\text{exogeneity}) \quad (9)$$

where i relates to the i -th vector element and the product process $(\xi_t Z_{it})_{(t=1, \dots, T)}$ is weakly stationary.³ Using (7), (8) and (9), we have

$$E[u_t Z_{1t}] = E[\tilde{R}_{\cdot 1} \xi_{1t} Z_{1t} + \tilde{R}^* \xi_t^{1*} Z_{1t}] = \tilde{R}_{\cdot 1} E[\xi_{1t} Z_{1t}] = \tilde{R}_{\cdot 1} \phi_1, \quad (10)$$

which allows one to identify $\tilde{R}_{\cdot 1}$ up to an unknown scalar ϕ_1 , i.e., up to scale and sign.

Similar to [Lunsford \(2015\)](#), we identify this scalar by exploiting the unit L^2 -norm of the columns of the rotation matrix:

$$E[Z_{1t} u_t^\top] E[u_t Z_{1t}] = \phi_1 \tilde{R}_{\cdot 1}^\top \tilde{R}_{\cdot 1} \phi_1 = \phi_1^2 \quad (11)$$

³By assuming covariance stationarity instead of mean-stationarity we can apply non-restrictive weak laws of large numbers to show the consistency of our estimator.

Thus, by inserting (11) into (10), we obtain:

$$\tilde{R}_{\cdot 1} = \pm E[u_t Z_{1t}] \left(E[Z_{1t} u_t^\top] E[u_t Z_{1t}] \right)^{-1/2}. \quad (12)$$

In (12), the sign is determined by the covariance of the instrumental variable and the structural shock of interest, i.e. by ϕ_1 . By orthogonality of rotation matrices, we can infer the structural shock of interest as

$$(\tilde{R}_{\cdot 1})^\top u_t = \xi_{1t}. \quad (13)$$

Likewise, we can infer the first column $Q_{\cdot 1,t}$.

2.3 A general recurrence scheme for full identification

Due to (5), the entire rotation matrix of a bivariate system is identified with a single proxy variable. In order to identify the full rotation matrix in an n -dimensional system, one could proceed in a similar fashion by simultaneously estimating all columns with $n - 1$ instruments by means of (12). Instead, we suggest a scheme which exploits that n -dimensional rotations can be expressed as sequences of Givens rotations. The identification approach via Givens rotations guarantees orthogonality of the structural shocks. This is of importance, because it is a priori not clear which proxy variables deliver orthogonal shocks and the exogeneity assumption (9) is not testable in advance. In contrast to identification column-by-column, our approach delivers a parametrization of the rotation matrix which offers further insights in its own right: For instance, because one obtains a set of rotation angles, one may study the relations between pairs or subsets of structural shocks. Moreover, it allows one to combine the proxy-based identification easily with other restrictions (see e.g. Fisher and Huh (2019)) to achieve full identification. When aiming at partial identification in larger dimensional systems, our strategy is well-

defined even if one can identify only a subset of columns of \tilde{R} .⁴

In the following paragraphs, we present the recurrence scheme for full identification of the angles of a rotation matrix of order $n \in \mathbb{N}_{\geq 2}$. In this case, $\frac{n(n-1)}{2}$ restrictions are sufficient and necessary for identification, because every rotation in a n -dimensional space can be expressed as a composition of $\frac{n(n-1)}{2}$ elemental rotations. Geometrically, these elemental rotations, called Givens rotations, correspond to sequences of rotations taking place in two-dimensional planes that are embedded in the n -dimensional space. The $\binom{n}{2}$ ways to position two-dimensional planes in \mathbb{R}^n correspond to the postulated $\frac{n(n-1)}{2}$ elemental rotations. Let θ_{ij} denote the angle of rotation in direction of axis x_j in the embedded plane in \mathbb{R}^n spanned by the axes x_i, x_j ($i, j \in \{1, \dots, n\}, i \neq j$). The rotation in this plane can be expressed by the $(n \times n)$ rotation matrix R^{ij} :

$$R^{ij}(\theta_{ij}) = \{r_{k,l}\}_{(k,l=1,\dots,n)} \text{ where } \begin{cases} r_{ii} &= \cos(\theta_{ij}) \\ r_{ij} &= -\sin(\theta_{ij}) \\ r_{ji} &= \sin(\theta_{ij}) \\ r_{jj} &= \cos(\theta_{ij}) \\ r_{kk} &= 1 & (k \neq i, j) \\ r_{kl} &= 0 & (\text{otherwise}), \end{cases} \quad (14)$$

i.e., an elemental rotation holds all dimensions – apart from i, j . The convention of each angle representing a rotation about a distinct fixed axis is commonly referred to as a Tait-Bryan system. It makes our calculations tractable as we always keep at least one dimension fixed. For a positive angle $\theta_{ij} > 0$, the elemental rotation occurs counterclockwise.

⁴The use of Givens rotations has not been coupled with a proxy-based and full identification strategy to date. This is partly due to the fact that, if the structural shocks are correlated with several proxies, there still exists an identification problem, now on the level of the structural shocks (Jentsch and Lunsford, 2019; Arias et al., 2021) which requires additional restrictions to be solved (see Angelini and Fanelli (2019) in the SVAR context).

Intuitively, the inverse of the corresponding rotation matrix corresponds to a clockwise rotation in the subplane by the same angle. We perform rotations both in counterclockwise and clockwise directions, when facing the positive direction of an axis, such that all rotation angles can be positive and negative. This is especially convenient in an economic application as it allows the rotation matrix to deviate in both angle directions from the identity matrix as an initial state where volatility transmission and reception between assets are symmetric.

Any rotation \tilde{R} in \mathbb{R}^n can be expressed as a continuous and differentiable composition of these elemental rotation matrices (Hoffman et al. (1972)). For the present work, we specify this composition as

$$\begin{aligned}\tilde{R} &= \prod_{i=1}^{n-1} \prod_{j=i+1}^n R^{ij}(\theta_{ij}) \\ &= R^{12}(\theta_{12}) \cdots R^{1n}(\theta_{1n}) R^{23}(\theta_{23}) \cdots R^{n-1,n}(\theta_{n-1,n}).\end{aligned}\tag{15}$$

Note that this is just one possible composition of elemental rotations. As matrix multiplication is non-commutative, the order of the elemental rotations has to be predetermined to ensure uniqueness of the estimated rotation angles; in other words, it is an econometric identification condition. It has, however, no economic implications, because one always rotates through all two-dimensional mutually orthogonal subplanes. The ordering principle we adopt in (15) ensures that the composition of the antecedent $\frac{m(m-1)}{2}$ elemental rotations forms an m -dimensional rotation ($m \in \mathbb{N}_{\leq n}$) for reasons, which we illustrate in Section 2.4.

To outline the n -dimensional case to infer unique rotation angles, denote the cosine (sine) evaluated at an angle θ_{ij} by c_{ij} (s_{ij}). We assemble the $\frac{n(n-1)}{2}$ angular parameters θ_{ij} , ($i =$

$1, \dots, n-1, j = i+1, \dots, n$), in the angular parameter matrix Θ given by

$$\Theta = \begin{pmatrix} 0 & \theta_{12} & \theta_{13} & \dots & \dots & \theta_{1n} \\ \vdots & 0 & \theta_{23} & \theta_{24} & \dots & \theta_{2n} \\ \vdots & \vdots & \ddots & \ddots & \dots & \vdots \\ \vdots & \vdots & \dots & \ddots & \ddots & \vdots \\ 0 & 0 & \dots & \dots & 0 & \theta_{n-1,n} \end{pmatrix} \quad (16)$$

The $\frac{n(n-1)}{2}$ angles θ_{ij} , ($i = 1, \dots, n-1, j = i+1, \dots, n$) describing an n -dimensional rotation \tilde{R}^{nD} with $n \in \mathbb{N}_{\geq 2}$ can be found by the following recursive approach:

For the angles θ_{ij} , with $i = 1, \dots, n-2$ and $j = i+2, \dots, n$, marked in (16) in red, it holds that

$$\begin{aligned} s_{in} &= \tilde{R}_{ni}^{((n-i+1)D)} \\ s_{ij} &= \tilde{R}_{ji}^{((n-i+1)D)} / (c_{i,(j+1)} \cdots c_{in}) \end{aligned} \quad (17)$$

where the angles are in $[-\frac{\pi}{2}, \frac{\pi}{2}]$; the remaining $(n-1)$ angles $\theta_{i,(i+1)}$, marked in blue have domain $[-\pi, \pi)$ and can be found from:⁵

$$\begin{aligned} s_{i,(i+1)} &= \tilde{R}_{i+1,i}^{((n-i+1)D)} / (c_{i,(i+2)} \cdots c_{in}) \\ c_{i,(i+1)} &= \tilde{R}_{ii}^{((n-i+1)D)} / (c_{i,(i+2)} \cdots c_{in}). \end{aligned} \quad (18)$$

If any angle $\theta_{i,k}$ in the denominator of (17) or (18) is equal to $-\frac{\pi}{2}$ all subsequent angles listed in this row of Θ can be chosen arbitrarily due to the loss of one degree of freedom in the angular parameters. At the parameter boundaries of the bluish angles with domains $[-\pi, \pi)$ we experience singularities where bijectivity and continuity of the map between the space of rotations and the angle parameter space fails.⁶ While the existence of discontinuities in the Givens representation may seem troubling, the singularities can

⁵For a derivation of the angular parameter domains, see Hoffman et al. (1972) but note that the ordering principle of the elemental rotations differs.

⁶For example, the inverse map from the space of two-dimensional rotations to $[-\pi, \pi)$ features a discontinuity at $F = \begin{pmatrix} -1 & 0 \\ 0 & -1 \end{pmatrix}$, because both $R^{12}(-\pi)$ and $\lim_{\theta \rightarrow \pi} R^{12}(\theta)$ converge to F .

always be shifted by using a different angle parameterization scheme due to the cyclical property of rotations. More generally, instead of viewing the angle parameter space as an n -dimensional interval in the Euclidean space, it is more convenient to view it in a topology which results from “glueing” opposite faces of the n -dimensional interval where the singularities occur together. In this new topology, they are thus removable.⁷

Instead of (17) and (18), the determination of the angles can be completed as well by the following scheme, which is numerically preferable if a two-argument arctan function, which returns values lying in the specified angle domains and takes into account signs, is available.⁸ In this case, the angles $\theta_{i,(i+1)}$ ($i = 1, \dots, n - 1$) ($\theta_{i,(i+1)} \in [-\pi, \pi$) are recovered from

$$\begin{aligned}\tan(\theta_{i,(i+1)}) &= \tilde{R}_{i+1,i}^{(n-i+1)D} / \tilde{R}_{ii}^{(n-i+1)D} \\ \text{sign}(s_{i,(i+1)}) &= \text{sign}\left(\tilde{R}_{i+1,i}^{(n-i+1)D}\right) \\ \text{sign}(c_{i,(i+1)}) &= \text{sign}\left(\tilde{R}_{ii}^{(n-i+1)D}\right)\end{aligned}\tag{19}$$

and $\theta_{ij} \in \left[-\frac{\pi}{2}, \frac{\pi}{2}\right)$ with $i = 1, \dots, n - 1$ and $j = i + 2, \dots, n$ follow from

$$\begin{aligned}\tan(\theta_{ij}) &= \left(\tilde{R}_{ji}^{(n-i+1)D} s_{i,(j-1)}\right) / \tilde{R}_{(j-1),i}^{(n-i+1)D} \\ \text{sign}(s_{ij}) &= \text{sign}\left(\tilde{R}_{ji}^{(n-i+1)D}\right).\end{aligned}\tag{20}$$

Similarly to the previous setting, if any term $s_{i,(j-1)}$ should be equal to $\tilde{R}_{(j-1),i}^{(n-i+1)D}$ all subsequent entries $\tilde{R}_{k,i}^{(n-i+1)D}$, $k = j, \dots, n$ cannot be determined and the remaining angles θ_{ik} in this row of Θ are set to zero.

In summary, all $\frac{n(n-1)}{2}$ angles determining the n -dimensional rotation matrix can be identified if parts of the full rotation matrix as compositions of elemental rotations are known. Given either a rotation matrix or a set of rotations angles, we can reconstruct the corresponding angular or matrix representation. This implies that the availability of $(n - 1)$

⁷In reference to the example in footnote 6, this corresponds to connecting the limit points by bending the interval line into a circle.

⁸Such a function is available in Matlab under the name “atan2.”

instruments allows for construction of the n -dimensional rotation matrix. We lay out the estimation strategy in Section 2.5.

2.4 Illustrative example

For illustration, we give here the rotation matrix and their decomposition into elemental matrices in four-dimensional case explicitly. According to (15), the four-dimensional rotation is described by

$$\tilde{R}^{(4D)} = \prod_{i=1}^3 \prod_{j=i+1}^4 R^{ij}(\theta_{ij}) = R^{12}R^{13}R^{14} \underbrace{R^{23}R^{24}}_{=\tilde{R}^{(2D)}} \underbrace{R^{34}}_{=\tilde{R}^{(3D)}} \underbrace{\hspace{1cm}}_{=\tilde{R}^{(4D)}} \quad (21)$$

such that it nests all lower-dimensional rotations in descending order. It is given explicitly by:

$$\begin{aligned} \tilde{R}^{(4D)} &= R^{12}R^{13}R^{14}R^{23}R^{24}R^{34} \\ &= \begin{pmatrix} c_{12} & -s_{12} & 0 & 0 \\ s_{12} & c_{12} & 0 & 0 \\ 0 & 0 & 1 & 0 \\ 0 & 0 & 0 & 1 \end{pmatrix} \begin{pmatrix} c_{13} & 0 & -s_{13} & 0 \\ 0 & 1 & 0 & 0 \\ s_{13} & 0 & c_{13} & 0 \\ 0 & 0 & 0 & 1 \end{pmatrix} \begin{pmatrix} c_{14} & 0 & 0 & -s_{14} \\ 0 & 1 & 0 & 0 \\ 0 & 0 & 1 & 0 \\ s_{14} & 0 & 0 & c_{14} \end{pmatrix} \\ &\quad \begin{pmatrix} 1 & 0 & 0 & 0 \\ 0 & c_{23} & -s_{23} & 0 \\ 0 & s_{23} & c_{23} & 0 \\ 0 & 0 & 0 & 1 \end{pmatrix} \begin{pmatrix} 1 & 0 & 0 & 0 \\ 0 & c_{24} & 0 & -s_{24} \\ 0 & 0 & 1 & 0 \\ 0 & s_{24} & 0 & c_{24} \end{pmatrix} \begin{pmatrix} 1 & 0 & 0 & 0 \\ 0 & 1 & 0 & 0 \\ 0 & 0 & c_{34} & -s_{34} \\ 0 & 0 & s_{34} & c_{34} \end{pmatrix} \\ &= R^{12}R^{13}R^{14} \begin{pmatrix} 1 & 0 & 0 & 0 \\ 0 & c_{23}c_{24} & -c_{34}s_{23} - c_{23}s_{24}s_{34} & -c_{23}c_{34}s_{24} + s_{23}s_{34} \\ 0 & c_{24}s_{23} & c_{23}c_{34} - s_{23}s_{24}s_{34} & -c_{34}s_{23}s_{24} - c_{23}s_{34} \\ 0 & s_{24} & c_{24}s_{34} & c_{24}c_{34} \end{pmatrix} \quad (22) \end{aligned}$$

$$= \begin{pmatrix} c_{12}c_{13}c_{14} & * & * & * \\ c_{13}c_{14}s_{12} & * & * & * \\ c_{14}s_{13} & * & * & * \\ s_{14} & c_{14}s_{24} & c_{14}c_{24}s_{34} & c_{14}c_{24}c_{34} \end{pmatrix}$$

where we keep those entries which allow for the straightforward identification of the angle parameters associated with the first column of the rotation matrix. The domains of $\theta_{12}, \theta_{23}, \theta_{34}$ are $[-\pi, \pi)$ and $[-\frac{\pi}{2}, \frac{\pi}{2})$ for all others. Clearly, knowing the first column of the rotation matrix, $\tilde{R}_{\cdot 1}^{(4D)}$, allows one to infer θ_{12}, θ_{13} and θ_{14} .

2.5 Estimation strategy

Let the asset system $(\varepsilon_t)_{t \in I}$ in \mathbb{R}^n and assume that instruments $Z_{1t}, \dots, Z_{n-1,t}$ are given for the first $(n-1)$ components of ξ_t . The estimation strategy is summarized in 1:

Algorithm 1:

Result: full n -dimensional rotation matrix

Initialization:

1. Estimate sequence of n -dimensional conditional covariance matrices $(H_t)_{t \in I}$;
2. Compute principal square roots $(\tilde{Q}_t)_{t \in I}$ and standardized residuals $(u_t)_{t \in I}$;

for $(i = 1, \dots, n-1)$: **do**

1. Estimate $\tilde{R}_{\cdot i}^{((n-i+1)D)}$ using Z_{ij} ;
2. Solve for $(n-i)$ rotation angles and obtain transition matrix D_{n-i+1} ;
3. Standardize $\tilde{R}_{\cdot i}^{((n-i+1)D)}$ with D_{n-i+1} ;

end

Use obtained angles to compute full n -dimensional rotation matrix.

We illustrate the algorithm for $i = 1$: We start by estimating $\tilde{R}_{\cdot 1}$. Knowledge of $\tilde{R}_{\cdot 1}$ provides us with the solutions to the first $(n-1)$ rotation angles, which are contained in

the matrix D_n below:

$$\tilde{R}^{(nD)} = \underbrace{R^{12} \dots R^{1n}}_{:=D_n} \cdot \underbrace{R^{23} \dots R^{n-2,n-1} R^{n-2,n} R^{n-1,n}}_{:=\tilde{R}^{(n-1)D}}$$

Here, $\tilde{R}^{((n-1)D)}$ has the structure:

$$\tilde{R}^{((n-1)D)} = \begin{pmatrix} 1 & 0 & \dots & 0 \\ 0 & * & \dots & * \\ \vdots & \vdots & \dots & \vdots \\ 0 & * & \dots & * \end{pmatrix}$$

In case of a violation of (9), we observe a non-zero first entry in the second column of $\tilde{R}^{((n-1)D)}$. We estimate the second column of $\tilde{R}^{(nD)}$ using the second proxy variable. As a composition of elemental rotations, D_n is a rotation matrix and thus invertible, hence multiplication with the inverse of D_n yields

$$\Leftrightarrow D_n^{-1} \tilde{R}^{(nD)} = \underbrace{R^{23} \dots R^{n-3,n} R^{n-2,n} R^{n-1,n}}_{:=\tilde{R}^{(n-1)D}} \quad (23)$$

Focusing on the second column, we obtain

$$D_n^{-1} \tilde{R}_{\cdot 2}^{(nD)} = \tilde{R}_{\cdot 2}^{((n-1)D)} = (0, *, \dots, *)^\top$$

from which we infer the $(n-2)$ rotation angles θ_{ij} ($i=2, j=i+1, \dots, n$). We iteratively continue these steps, until we arrive at the two-dimensional subsystem in the lower right corner, from which we derive the last angle $\theta_{n-1,n}$.

2.5.1 Estimation and consistency

Without loss of generality, we consider the estimation of the first column of an n -dimensional rotation matrix \tilde{R} . Let $z_1 = (z_{11}, \dots, z_{1T})^\top$ be the vector of the observed Z_1 and let $\hat{u} = (\hat{u}_1, \dots, \hat{u}_T)$ denote the matrix of estimated standardized residuals of the n -dimensional asset return system. In order to estimate $\tilde{R}_{\cdot 1}$, we define the estimators of

(10) and (11) as

$$\hat{\psi}_1 := \widehat{\tilde{R}}_{\cdot 1} \phi = \frac{1}{T} \sum_{t=1}^T \hat{u}_t z_{1t} \quad (24)$$

and

$$\widehat{\phi^2} := \left(\frac{1}{T} \sum_{t=1}^T z_{1t} \hat{u}_t^\top \right) \left(\frac{1}{T} \sum_{t=1}^T \hat{u}_t z_{1t} \right) = (\hat{\psi}_1)^\top \hat{\psi}_1 \quad (25)$$

Then we obtain the estimator for $\tilde{R}_{\cdot 1}$ as

$$\widehat{\tilde{R}}_{\cdot 1} \pm \hat{\psi}_1 \left(\widehat{\phi^2} \right)^{-1/2} \quad (26)$$

The estimation procedure is repeated iteratively for all columns of the rotation matrix.

Let η denote the vector of parameters defining the dynamics of the conditional covariance matrix $H_t = H_t(\eta)$ and assume that H_t is a continuous function of the true parameter vector η_0 . Let $\hat{\eta}$ denote the corresponding estimator. In order to establish consistency of $\widehat{\tilde{R}}_{\cdot 1}$ we adopt the following assumptions:

Assumption 2.1.

- (a) $\hat{\eta} \xrightarrow{p} \eta_0$
- (b) $\frac{1}{T} \sum_{t=1}^T \xi_t z_{1t} \xrightarrow{p} \mathbb{E}[\xi_t Z_{1t}]$

where \xrightarrow{p} denotes convergence in probability.

Proposition 2.1. Under Assumption 2.1, we have: $\widehat{\tilde{R}}_{\cdot 1} \xrightarrow{p} \tilde{R}_{\cdot 1}$.

Proof. The continuous mapping theorem implies by (a) that $H_t(\hat{\eta}) \xrightarrow{p} H_t(\eta_0)$ as $T \rightarrow \infty$. Thus, the decomposition $\tilde{Q}_t(\hat{\eta})$ converges to $\tilde{Q}_t(\eta_0)$ because the usage of the unique positive definite principal square root as initial decomposition \tilde{Q}_t represents a (uniformly) continuous operation in the space of positive definite matrices. By another application of the continuous mapping theorem we obtain $\hat{u}_t = \tilde{Q}_t(\hat{\eta})^{-1} \varepsilon_t \xrightarrow{p} \tilde{Q}_t(\eta_0)^{-1} \varepsilon_t = u_t$. As

$u_t = \tilde{R}\xi_t$, it holds that $\frac{1}{T} \sum_{t=1}^T u_t z_{1t} = \frac{1}{T} \sum_{t=1}^T \tilde{R}\xi_t z_{1t} = \tilde{R} \frac{1}{T} \sum_{t=1}^T \xi_t z_{1t}$. By the continuous mapping theorem and assumption (b) $\frac{1}{T} \sum_{t=1}^T \hat{u}_t z_{1t}$ consistently estimates $E[u_t Z_{1t}] = \tilde{R}_1 \phi$. Consistency of the estimators (25) and (26) follows by another application of the continuous mapping theorem. Note that assumption (b) does not require imposing an iid assumption but allows for a certain degree of serial correlation through the choice of a suitable weak law of large numbers (WLLN). For instance, we can choose a WLLN for weakly stationary correlated sequences with $\lim_{T \rightarrow \infty} \frac{1}{T} \sum_{i=0}^T \text{cov}((\xi_t Z_{1t})(\xi_{t-i} Z_{1,t-i})) = 0$.⁹ □

Given the estimates, we can uniquely infer the corresponding rotation angles. Recall that this map features discontinuities at certain angle domain boundaries. The continuous mapping theorem is still applicable by characterizing continuity in terms of preimages of open sets and considering the angular parameter space in a topological sense by glueing those interval faces at which we experience singularities (see the angular parameters marked in blue in (16)) together. This removes the discontinuities in the new topology.¹⁰

2.5.2 Testing

To justify the structural modeling approach, we develop a test for departures from symmetric volatility spillovers as implied by the usage of the (non-structural) principal square root. We suggest a Wald test based on the estimated rotation matrix. When the volatility spillovers between the assets are in fact asymmetric, the estimated rotation matrix departs

⁹In the VAR literature it is common to impose $E[Z_{1t} u_{t-j}] = 0$ ($j \neq 0$). Should this condition not be satisfied, it can be recovered by regressing z_{1t} on u_t and using the residual of this regression as a proxy variable.

¹⁰For two-dimensional rotations this corresponds to interpreting the parameter interval as a circle; for three-dimensional rotations this corresponds to interpreting the parameter space as a cylinder; see e.g. Hemingway and O'Reilly (2018).

from the identity matrix of no rotation postulated under the null hypothesis.

To build an inference framework, we follow ideas of Brüggenmann et al. (2014, 2016) and Jentsch and Lunsford (2019). We adopt the following additional assumptions:

Assumption 2.2.

- (1) Let $x_t := (u_t^\top, Z_t^\top)^\top$, such that the $(2n - 1)$ -dimensional process $(x_t)_{t \in \mathbb{Z}}$ consists of the n -dimensional standardized residual series and the $(n - 1)$ dimensional instrument series, and assume that the product process $(u_t Z_t^\top)_{t \in \mathbb{Z}}$ is weakly stationary.
- (2) Let $\alpha_x(h) = \sup_{A \in \mathcal{F}_{-\infty}^t, B \in \mathcal{F}_{t+h}^\infty, (t \in \mathbb{Z})} |P(A \cap B) - P(A)P(B)|$, $h \in \mathbb{N}$ denote the alpha-mixing coefficients of the process $(x_t)_{t \in \mathbb{Z}}$ where $\mathcal{F}_{-\infty}^t := \sigma(x_j : j \leq t)$ and $\mathcal{F}_{t+h}^\infty := \sigma(x_j : j \geq t + h)$. Assume furthermore that $\sup_t E \left[|x_t|_{2\beta}^{2\beta} \right] < \infty$ where $|M|_p = \left(\sum_{i,j} |m_{ij}|^p \right)^{1/p}$ for some matrix $M = (m_{ij})$ and let $\sum_{h \geq 1} \alpha_x(h)^{1 - \frac{2}{\beta}} < \infty$ for some $\beta > 2$.
- (3) Define the $(n \times n)$ matrices $\tau_h = E[(Z_{it} u_t)(Z_{i,t-h} u_{t-h})^\top]$ ($h \in \mathbb{Z}$) and assume that $V := \sum_{h=-\infty}^{+\infty} (\tau_h - \psi_i \psi_i^\top)$, where $\psi_i := \phi_i \tilde{R}_{\cdot i}$, exists and is positive definite.

The weak stationarity assumption (1) is needed to meet the relevance condition (8) and for the application of a suitable CLT. The summability condition in (2) ensures that $\alpha_x(h) \rightarrow 0$ as $h \rightarrow \infty$ such that the process $(x_t)_{t \in \mathbb{Z}}$ is said to be α -mixing. The mixing condition allows for general forms of serial dependence, for example for conditional heteroscedasticity. In particular, neither the standardized residuals nor the proxy variables must be iid. Assumption (3) guarantees the existence and positive definiteness of the asymptotic variance of our estimator. Note that the summability condition and the moment condition in (2) are sufficient to prove the existence of V by Davidson (1994, Corollary 14.3).

Proposition 2.2. Let $\psi_i := \phi_i \tilde{R}_{\cdot i}$ and define $\tilde{\psi}_i := \widetilde{\phi_i \tilde{R}_{\cdot i}} = \frac{1}{T} \sum_{t=1}^T u_t Z_{it}$. Under Assumption 2.2, we have

$$\sqrt{T}(\tilde{\psi}_i - \psi_i) \xrightarrow{d} N(0, V)$$

where \xrightarrow{d} denotes convergence in distribution.

Proof. To prove this CLT result under α -mixing assumptions on $(x_t)_{t \in \mathbb{Z}}$ we use the CLT of Herrndorf (1984) (see Francq and Zakoian (2010, Theorem A.4)) generalized to random vectors by means of a Cramér-Wold device (see Davidson (1994, Theorem 25.5 & 25.6)). Let $\lambda \in \mathbb{R}^n$ such that $\|\lambda\| = 1$ and define $\Lambda_{it} = \lambda^\top \iota_{it}$ where $\iota_{it} := u_t Z_{it} - \psi_i$. By the moment boundedness condition on $(x_t)_{t \in \mathbb{Z}}$ in (2), the univariate process $(\Lambda_{it})_{t \in \mathbb{Z}}$ satisfies $\sup_t E[|\Lambda_{it}|^\beta] < \infty$ for some $\beta > 2$. Furthermore, Davidson (1994, Theorem 14.1) implies that the α -mixing coefficients $(\alpha_\Lambda(h), h \in \mathbb{N})$ of the process $(\Lambda_{it})_{t \in \mathbb{Z}}$ decay at the same rate as $(\alpha_x(h), h \in \mathbb{N})$ of the process $(x_t)_{t \in \mathbb{Z}}$, such that we have $\sum_{h \geq 1} \alpha_\Lambda(h)^{1 - \frac{2}{\beta}} < \infty$ by the summability condition in Assumption 2.2. Together with the assumptions in (3) we can apply the CLT of Herrndorf (1984) in combination with the Cramér-Wold theorem. The limiting variance of $\sqrt{T}(\tilde{\psi}_i - \psi_i)$ is given by

$$\begin{aligned} \text{Var} \left(\frac{1}{\sqrt{T}} \sum_{t=1}^T \iota_{it} \right) &= \frac{1}{T} \sum_{h=-(T-1)}^{T-1} \sum_{t=\max(1, 1+h)}^{\min(T, T+h)} \text{cov}(\iota_{it}, \iota_{i, t-h}) \\ &\rightarrow \sum_{h=-\infty}^{+\infty} \text{cov}(Z_{it} u_t, Z_{i, t-h} u_{t-h}) = \sum_{h=-\infty}^{+\infty} (\tau_h - \psi_i \psi_i^\top) \end{aligned}$$

as $T \rightarrow \infty$ which completes the proof. \square

To conduct the Wald test for departures from symmetric spillovers, we use Proposition 2.2 to derive the limiting distribution of the estimated rotation matrix in Corollary 2.1.

Corollary 2.1. Under Assumption 2.2, we have:

$$\sqrt{T}(\hat{R}_{\cdot i} - \tilde{R}_{\cdot i}) \xrightarrow{d} N(0, W)$$

where $W = M_\psi V M_\psi^\top$ and $M_\psi := -\psi_i (\psi_i^\top \psi_i)^{-\frac{3}{2}} \psi_i^\top + (\psi_i^\top \psi_i)^{-\frac{1}{2}} I_n$.

Proof. As $\tilde{R}_{\cdot i}$ is a smooth function of ψ_i , which is by assumption not the zero vector, we can apply the Delta method to obtain the asymptotic covariance matrix of the estimators

of the rotation matrix. To derive M_ψ , rewrite the estimator as

$$\begin{aligned}\widetilde{\mathbf{R}}_{\cdot,i} &= \pm \left(\frac{1}{T} \sum_{t=1}^T \hat{u}_t z_{it} \right) \left[\left(\frac{1}{T} \sum_{t=1}^T z_{it} \hat{u}_t^\top \right) \left(\frac{1}{T} \sum_{t=1}^T \hat{u}_t z_{it} \right) \right]^{-1/2} \\ &= \pm \widetilde{\boldsymbol{\psi}}_i \left(\widetilde{\boldsymbol{\psi}}_i^\top \widetilde{\boldsymbol{\psi}}_i \right)^{-\frac{1}{2}}\end{aligned}$$

Then M_ψ is given by:

$$\begin{aligned}M_\psi &:= \frac{\partial \widetilde{\mathbf{R}}_{\cdot,i}}{\partial \boldsymbol{\psi}_i^\top} = \pm \left(-\frac{1}{2} \boldsymbol{\psi}_i (\boldsymbol{\psi}_i^\top \boldsymbol{\psi}_i)^{-\frac{3}{2}} (\boldsymbol{\psi}_i^\top (I_n + I_n)) + (\boldsymbol{\psi}_i^\top \boldsymbol{\psi}_i)^{-\frac{1}{2}} I_n \right) \\ &= \pm \left(-(\boldsymbol{\psi}_i^\top \boldsymbol{\psi}_i)^{-\frac{3}{2}} \boldsymbol{\psi}_i \boldsymbol{\psi}_i^\top + (\boldsymbol{\psi}_i^\top \boldsymbol{\psi}_i)^{-\frac{1}{2}} I_n \right).\end{aligned}$$

□

This result allows us to formulate a Wald test to check whether the estimated rotation matrix departs from the identity matrix by restricting the off-diagonal elements of the first $(n - 1)$ columns of the rotation matrix to be zero.

Practically, the test is based on \hat{u}_t rather than u_t . We therefore incur an additional error that is due to estimating η by the QML method. Unfortunately, it appears quite difficult to account for this additional sampling variation. However, our empirical evidence is sufficiently compelling to leave room for robustness under an inflated asymptotic variance due to sampling variability of the BEKK parameters. We estimate the asymptotic covariance matrix by means of a Newey-West heteroscedasticity and autocorrelation robust estimator with automatic lag length selection and thus account for heteroscedasticity and serial correlation of unknown forms.

3 MGARCH model

Let the process $(\xi_t)_{t \in \mathbb{Z}} \subseteq \mathbb{R}^n$ denote an n -dimensional real-valued strict white noise process with zero mean and unit covariance matrix, i.e. $\xi_t \sim \text{SWN}(0, I_n)$. The process $(\varepsilon_t)_{t \in \mathbb{Z}}$

follows a strong MGARCH process if it satisfies:

$$\varepsilon_t = H_t^{1/2} \xi_t \quad (t \in \mathbb{Z}). \quad (27)$$

Here, $H_t^{1/2} \in \mathbb{R}^{n \times n}$ denotes a decomposition of the form $H_t^{1/2} (H_t^{1/2})^\top = H_t$ of the sequence of positive definite matrices $(H_t)_{t \in \mathbb{Z}}$. The process $(H_t)_{t \in \mathbb{Z}}$ is covariance stationary and measurable with respect to the filtration $\mathcal{F}_{t-1} = \sigma(\{\varepsilon_s : s \leq t-1\})$, $(\varepsilon_t)_{(t \in \mathbb{Z})}$ is a multivariate martingale difference with $E[\varepsilon_t | \mathcal{F}_{t-1}] = 0$ ($E[|\varepsilon_t|] < \infty$) and its conditional covariance matrix is given by $\text{Var}[\varepsilon_t | \mathcal{F}_{t-1}] = H_t$. In order to specify the conditional dynamics of the process, various specifications have been proposed, among which the parametric VEC and BEKK GARCH models enjoy great popularity (Bauwens et al., 2006). The BEKK GARCH model of Engle and Kroner (1995) ensures positive definiteness of H_t by construction. The n -dimensional process $(\varepsilon_t)_{t \in \mathbb{Z}}$ admits a BEKK(p, q) specification if H_t satisfies for all $t \in \mathbb{Z}$:

$$H_t = CC^\top + \sum_{i=1}^p A_i^\top \varepsilon_{t-i} \varepsilon_{t-i}^\top A_i + \sum_{j=1}^q B_j^\top H_{t-j} B_j \quad (p, q \in \mathbb{N}) \quad (28)$$

where C is a lower triangular matrix and A_i and B_j are coefficient matrices in $\mathbb{R}^{n \times n}$. The intercept matrix CC^\top is by construction symmetric and positive definite if C has full rank. The latter ensures positive definiteness of $(H_t)_{t \in \mathbb{Z}}$. Boussama et al. (2011, Theorem 2.4) show that under weak regularity conditions on $(\xi_t)_{(t \in \mathbb{Z})}$, the MGARCH process is ergodic, strictly and weakly stationary and invertible if the eigenvalues of $\sum_{i=1}^p A_i \otimes A_i + \sum_{j=1}^q B_j \otimes B_j$ are less than one in modulus. Hafner and Preminger (2009) provide conditions to establish consistency as well as asymptotic normality of the QML estimator assuming i.a. existence of second-order moments of $(\xi_t)_{(t \in \mathbb{Z})}$ and finite sixth-order moments of $(\varepsilon_t)_{t \in \mathbb{Z}}$. The MGARCH model thus fulfills the requirements for identification postulated in Section 2.5.1. Due to the quadratic structure of the BEKK(p, q) model, the parameter matrices are only identified up to sign. The BEKK(1, 1) model is uniquely identified if we assume the diagonal elements of C and the first matrix entries of $A_1, a_{11(1)}$, and $B_1, b_{11(1)}$, to be positive.

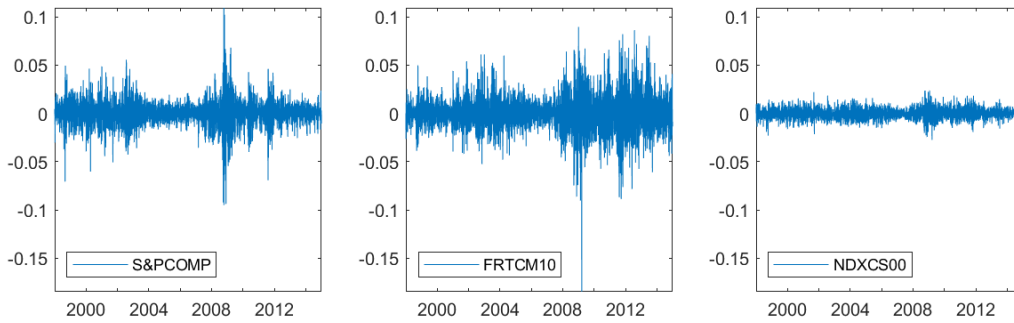


Figure 1: Demeaned daily log returns of the S&P 500 Composite Index (SP500), the yield of the U.S. constant maturity 10 year treasury note (FRTCM10) and the Finex U.S. Dollar Index (NDXCS00) from 1/1/1998 to 12/31/2014.

4 An identified asset return system

In this section, we illustrate the structural proxy-MGARCH approach by analyzing a system of daily returns covering three major asset classes: equity, fixed income and the foreign exchange markets. These are the most important asset classes for portfolio optimization and the key ingredients of the composite indicator of systemic stress in the financial system employed by the ECB (Kremer et al., 2012).

4.1 Data

We study daily price data ranging from 1/1/1998 to 12/31/2014 taken from Bloomberg. Our asset triple consists of the S&P 500 Composite Index (SP500), the yield of the U.S. constant maturity 10 year treasury note (FRTCM10) and the Finex U.S. Dollar Index (NDXCS00). The Finex is a measure of the value of the U.S. dollar relative to a currency basket of major U.S. trade partners. It increases when the U.S. dollar gains value compared to the other currencies. We compute daily log returns r_t for each asset; see Figure 1. All series exhibit the typical features of daily return data, such as heteroscedasticity and volatility clustering (see also the summary statistics in Table 1).

Statistic	SP500	FRTCM10	NDXCS00
Minimum	-0.0950	-0.1847	-0.0275
Maximum	0.1093	0.0895	0.0236
Mean	-0.0001	0.0000	-0.0000
Median	-0.0000	0.0002	-0.0000
Std. Dev.	0.0125	0.0176	0.0052
Skewness	-0.2033	-0.1360	-0.0343
Kurtosis	10.9287	8.4542	4.4914

Table 1: Descriptive statistics of the demeaned daily log returns of the S&P 500 Composite Index (SP500), the yield of the U.S. constant maturity 10 year treasury note (FRTCM10) and the Finex U.S. Dollar Index (NDXCS00) from 1/1/1998 to 12/31/2014; $N = 4435$ observations.

News data to proxy for the underlying structural shocks are taken from Thomson Reuters MarketPsych Indices (TRMI). Thomson Reuters process news and social media in real-time to construct economic indicators, among them sentiment indicators. The indicators are available for individual companies, economic sectors, geographical regions, countries, country markets, commodities and energy topics, indices as well as currencies. We use TRMIs for the U.S. as a geographical and political entity as well as the U.S. as an economic and financial marketplace. The TRMIs are available on a daily level. Only news items published until 3:30 pm Eastern time are taken into account by Thomson Reuters for the computation of the daily index values. This time window is not perfectly aligned with the end of the core trading session of the NYSE at 4:00 pm Eastern time, which determines the closing price. As the news measurement window ends thirty minutes before market close, we may miss information inherent to important news items published during the last thirty minutes of the core trading session, which may weaken our proxy. However, the misalignment precludes a forward-looking bias of our proxy variables.

With regard to proxy variable selection, natural candidates are the U.S. stock index sen-

Statistic	stock index sentiment	bond sentiment
Minimum	-3.1342	-4.8296
Maximum	3.3754	5.5997
Mean	-0.0000	0.0000
Median	-0.0097	-0.0469
Std. Dev.	1.0000	1.0000
Skewness	0.0564	0.2383
Kurtosis	2.5325	4.2307

Table 2: Descriptive statistics for the standardized and filtered TRMI indices on trading days from 1/1/1998 to 12/31/2014; $N = 4435$ observations.

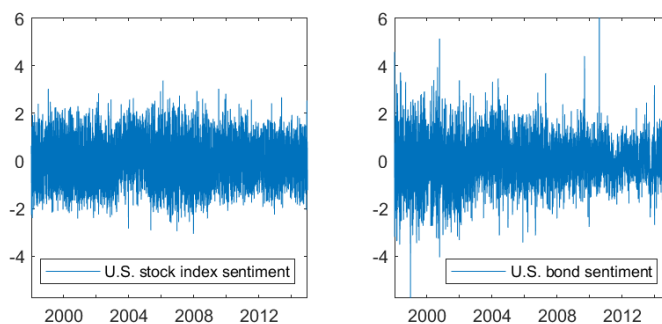


Figure 2: ARMA filtered and standardized U.S. stock index and bond sentiment on trading days from 1/1/1998 to 12/31/2014.

timent and the U.S. bond sentiment. The U.S. stock index sentiment is likely to reflect unexpected economic and political news concerning the S&P 500 and is thus expected to proxy for an equity market shock. Similarly, the bond market sentiment captures the perception of news about government bond markets and may thus proxy for a bond market shock. As bond prices move in opposite direction to bond yields, a structural shock identified by means of the bond market sentiment is expected to be connected to the treasury yield with inverted sign. It is vital to realize that the exogeneity condition imposed on proxies and structural shocks does not preclude that e.g. bond market news affect equity returns. While the structural rotation categorizes the standardized residuals into

identified structural shocks, the matrix square root of the conditional covariance matrix determines the mix of these shocks which makes up the individual asset returns.

With regard to the range of the TRMIs, a value of zero is interpreted as a neutral signal, negative values convey a negative signal and positive values a positive one. As our proxy variables are high-frequent, we do not face the difficulties stemming from proxy variables being censored at zero as is common in the proxy-SVAR literature. We fit flexible ARMA models to the series to distill the unexpected innovations to the proxy series. Table 2 shows statistical summary measures of the resulting indicators. Figure 2 shows the filtered and standardized proxy time series.

4.2 Structural model estimates

Table 3 documents the results of the QMLE of the full BEKK on the asset return system. By using the values of a diagonal BEKK model as starting values combined with a randomization strategy for the off-diagonal elements of the coefficient matrices, we verify that the resulting estimates correspond to a maximum of the loglikelihood function. We optimize the loglikelihood numerically using the analytical derivatives provided in [Hafner and Herwartz \(2008\)](#), while monitoring the spectral radius. Inference with regard to the coefficient matrices of the BEKK model is based on t-statistics derived from the analytical derivatives. The diagonal parameters and selected off-diagonal parameters of the coefficient matrices turn out to be statistically significant at conventional levels. The Akaike criterion speaks in favor of the full BEKK specification (see Table 3) such that we base our further analysis on the latter model.

The analysis of the proxy variables reveals that the stock market index and bond market sentiment seem to be relevant instruments; see Table 4. The inferred rotation angles

lie in the interior of the angular parameter space. They are clearly different from zero causing the structural rotation matrix to depart from the identity matrix. This indicates that spectral decompositions imposing symmetric spillover mechanisms are not applicable. The Wald test confirms this finding; see Table 4. The correlation matrix of the inferred structural shocks with the proxy variables shows a diagonal structure in agreement with the relevance (8) and the exogeneity condition (9) with p-values of zero indicating the statistical significance of the relation of the structural shocks of interest and their respective proxy variables. The inferred structural shocks are mutually and serially uncorrelated and seem to exhibit white noise properties (see Table 5).

	\hat{C}	\hat{A}	\hat{B}
0.0011	$3.04 \times 1e^{-6}$	$-2.98 \times 1e^{-6}$	0.2677
-	$8.92 \times 1e^{-4}$	$1.04 \times 1e^{-4}$	0.0003
-	-	$2.89 \times 1e^{-4}$	0.0631
(3.8683)	(0.0027)	(-0.0195)	(4.7720)
-	(2.9861)	(2.1167)	(0.0209)
-	-	(6.0328)	(1.3258)
			(0.1861)
			(0.0169)
			-0.0108
			0.9580
			0.0014
			-0.0120
			0.0102
			0.0029
			-0.0029
			0.9752
			-0.0008
			0.9883
			(-0.0840)
			(1.1631)
			(195.32)
			(-1.6027)
			(1.1362)
			(677.01)

Spectral radius: 0.9985

Akaike criterion

full BEK: -88661

DBEKK: -88639

Table 3: Quasi maximum likelihood (QML) parameter estimates of the unrestricted BEKK model of the demeaned daily log returns of the S&P 500 Composite Index (SP500), the yield of the U.S. constant maturity 10 year treasury note (FRTCM10) and the Finex U.S. Dollar Index (NDXCS00) over the time period from 1/1/1998 to 12/31/2014. Entries in parentheses are the robust QML t-ratios determined by means of the analytical derivatives as provided by Hafner and Herwartz (2008).

To substantiate the claim that our inferred model is indeed structural, we narratively corroborate the lower (upper)¹¹ 1%-quantiles of the structural shocks by extracting the major financial news of these days. The results are tabulated in Tables 6, 7 and 8. We can connect each structural shock to specific economic and financial turmoil events reported in the news. As Tables 6, 7 and 8 show, the structural shocks are associated with distinct categories of news. ξ_1 captures news related to global economic and political uncertainty affecting equity markets as well as the impact of unexpected events such as terrorist attacks. Moreover, it comprises news regarding the current and prospective financial solidity of big U.S. companies and sectors and reflects the outlook on U.S. economic activity. In addition, we find news items which debate the potential impact of interest rate changes on equity markets. Importantly, ξ_1 captures shocks related to the financial crisis of 2008 and the European debt crisis and, related to this, fiscal shocks such as sovereign rating changes.

The second structural market shock is driven almost exclusively by Fed announcements, inflation data and employment reports with a smaller part of news related to economic turmoil events threatening global economic prospects. It thus carries the flavor of a monetary policy and macroeconomic shock. The third shock vector captures all events relevant to the system which are not covered by the first two structural shocks. Whereas it does not have a structural interpretation a priori, our narrative corroboration reveals that the third shock does indeed reflect a certain category of news, namely events related to movements in the foreign exchange markets. While currency topics seem to dominate, we also observe connections to the gold price, energy and trade balance matters. Concretely, the upper 1%-quantile of the shock vector coincides largely with USD dips and oil or gold

¹¹Note that for the second and third shock the analysis is based on the upper 1%-quantile. This is due to the inverse relationship of bond prices and yields which implies a reversed sign in the associated structural shock vector. The sign of the last shock vector is a priori undetermined but can be inferred from the financial context for interpretation.

rallies, whereas the lower 1%-quantile correspondingly reflects jumps in the USD and USD strength especially against the EUR. Summarizing the discussion, we thus conclude that we identify ξ_1 as equity shock, ξ_2 as bond market shock and refer to ξ_3 as currency shock.

		proxy-MGARCH model		
$(\hat{\theta}_{12}, \hat{\theta}_{13}, \hat{\theta}_{23})^\top$		0.3811	-0.1885	-2.9164
\hat{R}		0.9118	0.3238	-0.2526
		0.3654	-0.9204	0.1393
		-0.1874	-0.2193	-0.9575
		ξ_1	ξ_2	ξ_3
correlations	Z_1	0.3347	0.0000	-0.0000
	Z_2	0.0052	0.1936	0.0000
t-statistics	Z_1	23.6478	0.0000	-0.0000
	Z_2	0.3469	13.1349	0.0000
p-values	Z_1	0	1.0000	1.0000
	Z_2	0.7286	0	1.0000
Wald test	distribution	statistic	critical value	p-value
symmetric spillovers	$\chi^2_{(4)}$	107.85	9.4877	0.0000

Table 4: Estimation results of the structural MGARCH model of the demeaned daily log returns of the S&P 500 Composite Index (SP500), the yield of the U.S. constant maturity 10 year treasury note (FRTCM10) and the Finex U.S. Dollar Index (NDXCS00) from 1/1/1998 to 12/31/2014 when using the stock market index (Z_1) and bond market sentiment (Z_2) TRMIs as proxy variables. The table shows, from top to bottom, the estimated rotation angles, the estimated rotation matrix and the correlations of the proxies with the inferred structural shocks ξ_1 , ξ_2 and ξ_3 including Wald test for symmetry of volatility spillovers.

proxy-MGARCH model			
Statistic	ξ_1	ξ_2	ξ_3
Mean	-0.0106	0.0023	0.0077
Median	0.0224	-0.0022	0.0117
Minimum	-7.2849	-4.6486	-4.3832
Maximum	3.6610	7.3030	5.4038
Std. Dev.	0.9903	1.0027	1.0006
Skewness	-0.4683	-0.0190	0.1615
Kurtosis	4.7569	5.0415	4.0728

Ljung-Box test for serial correlation			
Lag order	p-value ξ_1	p-value ξ_2	p-value ξ_3
$l = 5$	0.1631	0.0868	0.0769
$l = 10$	0.2133	0.1756	0.3679
$l = 15$	0.2607	0.1660	0.3881

Correlation			
	ξ_1	ξ_2	ξ_3
ξ_1	1.0000	0.0179	0.0171
ξ_2	0.0179	1.0000	-0.0242
ξ_3	0.0171	-0.0242	1.0000
p-values ξ_1	0	0.2331	0.2544
p-values ξ_2	0.2331	0	0.1068
p-values ξ_3	0.2544	0.1068	0

Table 5: Descriptive statistics of the inferred structural shocks of the structural MGARCH model of the demeaned daily log returns of the S&P 500 Composite Index (SP500), the yield of the U.S. constant maturity 10 year treasury note (FRTCM10) and the Finex U.S. Dollar Index (NDXCS00) from 1/1/1998 to 12/31/2014 using the stock market index and bond market sentiment as proxy variables.

4.3 Volatility spillovers

One of the most important application of MGARCH models is the analysis of volatility transmission mechanisms between several markets (Bauwens et al., 2006). Given the identified labeled structural shocks, we now analyze the volatility spillovers implied by these economically interpretable shocks. To this end, we define the following two measures for volatility reception and transmission. Let $i, j \in \{1, \dots, n\}$. Then volatility reception and transmission between i and j is measured by

$$VR_{t,i \leftarrow j} = \frac{q_{t,ij}^2}{\sum_{l=1}^k q_{t,il}^2} \quad (\text{volatility reception}) \quad (29)$$

$$VT_{t,i \rightarrow j} = \frac{q_{t,ij}^2}{\sum_{l=1}^k q_{t,lj}^2} \quad (\text{volatility transmission}) \quad (30)$$

where $q_{t,ij}$ denote the matrix entries of the identified Q_t . Volatility reception measures the share of the impact of the j -th structural shock on the i -th return in relation to the impact of all other shocks on this component. Volatility transmission measures the share of the impact of the i -th structural shock on the j -th return component in relation to its impact on all return components in the system. This definition follows a similar concept as the spillover measures defined by Diebold and Yilmaz (2012) and Fengler and Herwartz (2018) and can be understood as a 0-order forecast error variance decomposition.

Figures 3 and 4 show the volatility reception and transmission mechanisms implied by the structural model. We focus first on the reception mechanisms in Figure 3. Understandably, the equity shock contributes the most to S&P 500 return fluctuations, about 80% (see Figure 3a). The dominance becomes stronger since the financial crisis (2008) and remains elevated in the subsequent five years where the contribution amounts to up to 100%. While the equity shock accounts for the largest share in S&P 500 return fluctuations, the bond market shock shows notable contributions especially during calm market periods (see Figure 3b). This aligns well with Boyd et al. (2005), who finds evidence of

strong responses of the U.S. equity market to macroeconomic news dependent on the economic conditions. With regard to the relative influence of the currency shock on the S&P 500 returns, there seems to exist a relatively stable base level of volatility reception of around 7% paired with an absence of volatility reception during the quantitative easing efforts of the Fed (see Figure 3c).

Turning to the second row in Figure 3, we see that the return on the yield shows a comparably lower but pronounced volatility reception of on average if 20% coming from the equity shock (see Figure 3d). This reception strength increases in the course of the Dot-Com crisis from 2000 to 2003 from a level close to zero to almost 60%, before dropping to about 15% in 2003 and remaining stable until 2007. Subsequently, the link becomes strong again during the financial crisis (2007 - 2008) and the Euro zone crisis (2009 - 2014). Naturally, the bond market shock contributes the most to movements in the yield (see Figure 3e), whereas the currency shock exhibits almost no influence (see Figure 3f) on yield variations. The observation that currency shocks contribute little to the volatility of equity and bond returns aligns well with the findings, e.g., of Cenedese and Mallucci (2016).

Finally, the third row of Figure 3 depicts the volatility reception of the Finex return from the structural shocks. While the contribution of the equity shock to movements in the index returns is close to zero from 1998 to 2008, from the end of September 2008 to the end of May 2013 we observe a sudden surge in volatility reception to levels of 20% and more from the equity shock (see Figure 3g). The latter time span corresponds to a period of low interest rates reflecting the quantitative easing measures of the Fed and consequential depreciations of the USD. Figure 3h documents a relatively strong influence of the bond market shock on the Finex return which is in line with the finding by Andersen et al. (2003) that U.S. macroeconomic news has a significant effect on the USD - EUR exchange rate. According to Figure 3i the currency shock contributes the most to movements in the

returns. However, it seems to lose in terms of relative importance over the sample period with its contribution dropping from a level of close to 100% to around 80%.

Figure 4 documents the volatility transmission mechanisms. As a most striking observation we observe secular trends in volatility transmission between equity and fixed income markets (see Figures 4a and Figures 4d): The relative importance of the equity shock on the S&P 500 return decreases in relation to its impact on all return components in the system from approximately 80% to 50%, whereas the relative importance of the equity shock on the treasury yield increases simultaneously from 20% to a level around 50%. While we may find such observations natural in light of quantitative easing measures of the Fed, our analysis reveals that this trend started much before the financial crisis in 2008. This finding complements a strand of literature suggesting a strong link between fixed income and equity markets (Rigobon and Sack, 2003; Ehrmann et al., 2011).

The transmission mechanism from the bond market shock to the S&P 500 return weakens over time, decreasing from levels of around 10% at the turn of the millennium to close to zero by 2008; see Figure 4b. Figure 4e shows that this shift is mirrored in a stronger transmission of the bond market shock to the treasury yield return over time.

Finally, the currency shock exhibits a distinct volatility transmission pattern on each return component. We observe the strongest total shock contribution in Figure 4i. The transmission strength on the Finex return seems to fluctuate around a stable mean level of 70%. In contrast, we observe surges in transmission strength to the S&P 500 return from 1998 to 2004 and from 2006 to 2009. While the transmission level to the treasury yield returns is generally low at levels below 20%, it increases in the aftermath of the financial crisis, reaching a maximum of 60% during the Euro zone crisis in 2012. These observations support the interpretation of the third shock as a currency shock.

5 Conclusion

We have introduced a proxy-based structural MGARCH model which extends the reduced form GARCH model to a structural model in the macroeconomic sense. It guarantees flexible modeling of the multivariate volatility dynamics of returns and simultaneously identifies the underlying shock system and the shock propagation channels by delivering labeled structural shocks. Indeed, it is even possible to connect each shock component to specific news items and financial market events. Our identification strategy allows for full identification of the rotation angles of the structural rotation by means of a general recurrence scheme using Givens rotations which ensures orthogonality of the resulting shocks. In an empirical application to a system of equity, bond and foreign exchange returns, we obtain readily interpretable structural shocks and can reveal structural volatility reception and transmission patterns between the three markets. In particular, the volatility spillover mechanism departs from symmetric spillovers as implied by spectral decompositions as a typical ad hoc solution of the identification problem. The interpretation of the model-implied structural shocks can be narratively corroborated. Our structural approach to multivariate volatility modeling opens a pathway to further research. For example, it would be appealing to embed our approach in a large-dimensional MGARCH system which is driven by a small set of proxy-identified factors.

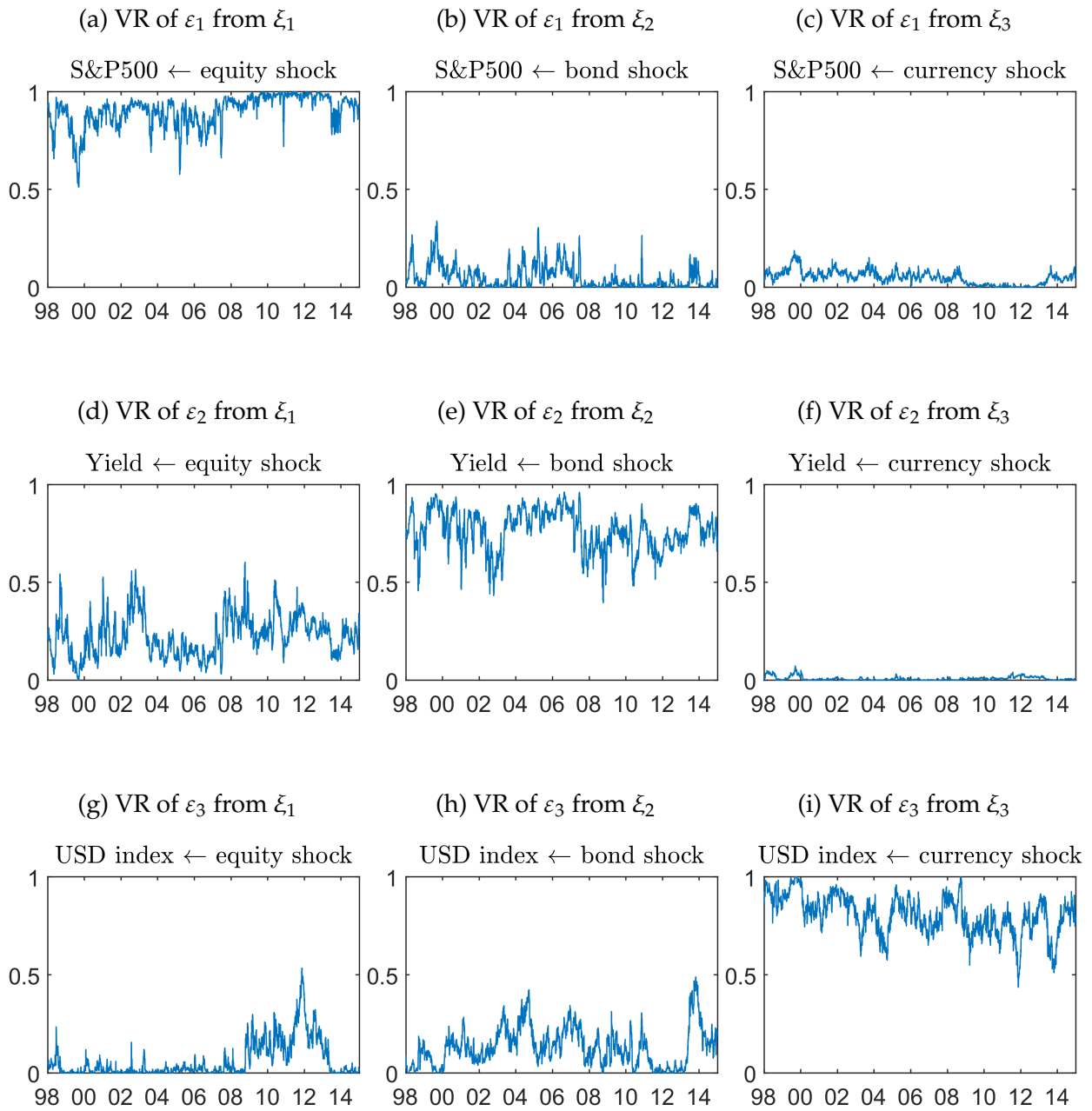


Figure 3: Volatility reception mechanisms of the structural MGARCH model of the de-meaned daily log returns of the S&P 500 Composite Index (SP500), the yield of the U.S. constant maturity 10 year treasury note (FRTCM10) and the Finex U.S. Dollar Index (NDXCS00) from 1/1/1998 to 12/31/2014 when using the stock market index (Z_1) and bond market sentiment (Z_2) TRMIs as proxy variables.

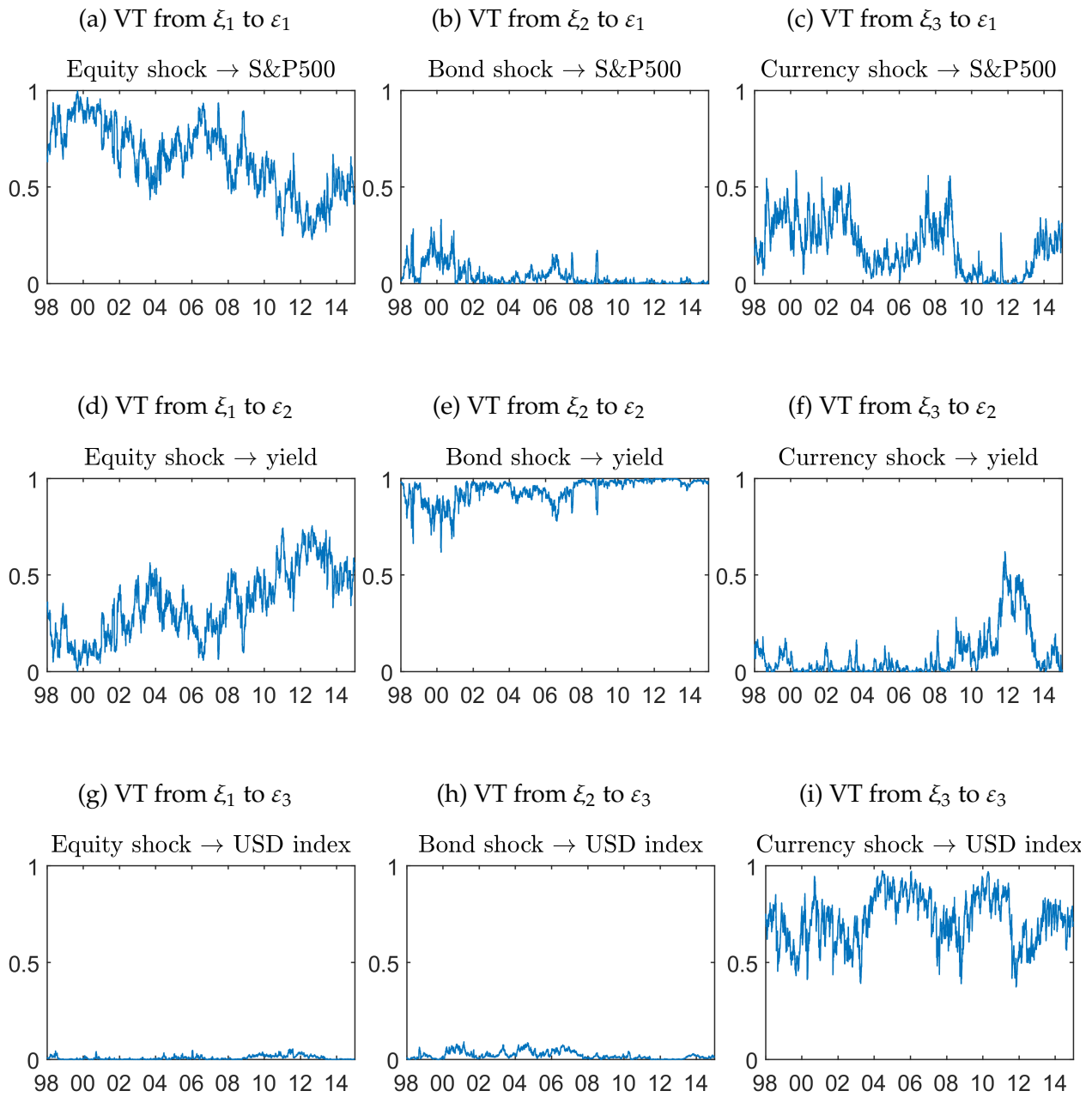


Figure 4: Volatility transmission mechanisms of the structural MGARCH model of the demeaned daily log returns of the S&P 500 Composite Index (SP500), the yield of the U.S. constant maturity 10 year treasury note (FRTCM10) and the Finex U.S. Dollar Index (NDXCS00) from 1/1/1998 to 12/31/2014 when using the stock market index (Z_1) and bond market sentiment (Z_2) TRMIs as proxy variables.

References

- Amisano, G. and Giannini, C. (1997). *Topics in Structural VAR Econometrics*, Springer, Berlin, Heidelberg.
- Andersen, T., Bollerslev, T. and Diebold, F. (2003). Micro effects of macro announcements: Real-time price discovery in foreign exchange, *American Economic Review* **93**: 38–62.
- Andersen, T. G., Davis, R. A., Kreiß, J.-P. and Mikosch, T. V. (2009). *Handbook of financial time series*, Springer Science & Business Media.
- Angelini, G. and Fanelli, L. (2019). Exogenous uncertainty and the identification of structural vector autoregressions with external instruments, *Journal of Applied Econometrics* **34**(6): 951–971.
- Arias, J. E., Rubio-Ramírez, J. F. and Waggoner, D. F. (2021). Inference in Bayesian proxy-SVARs, *Journal of Econometrics* .
- Bauwens, L., Hafner, C. and Laurent, S. (2012). *Handbook of Volatility Models and Their Applications*, John Wiley & Sons, Ltd.
- Bauwens, L., Laurent, S. and Rombouts, J. V. K. (2006). Multivariate GARCH models: a survey, *Journal of Applied Econometrics* **21**(1): 79–109.
- Bollerslev, T., Li, J. and Xue, Y. (2018). Volume, volatility, and public news announcements, *The Review of Economic Studies* **85**(4): 2005–2041.
- Boudoukh, J., Feldman, R., Kogan, S. and Richardson, M. (2018). Information, trading and volatility: Evidence from firm-specific news, *The Review of Financial Studies* **32**(3): 992–1033.
- Boussama, F., Fuchs, F. and Stelzer, R. (2011). Stationarity and geometric ergodicity of BEKK multivariate GARCH models, *Stochastic Processes and their Applications* **121**(10): 2331–2360.
- Boyd, J. H., Hu, J. and Jagannathan, R. (2005). The stock market’s reaction to unemployment news: Why bad news is usually good for stocks, *Journal of Finance* **60**(2): 649–672.
- Brüggemann, R., Jentsch, C. and Trenkler, C. (2014). Inference in VARs with conditional heteroskedasticity of unknown form. Working Paper 2014-13, Department of Economics, University of Konstanz.
- Brüggemann, R., Jentsch, C. and Trenkler, C. (2016). Inference in VARs with conditional heteroskedasticity of unknown form, *Journal of Econometrics* **191**(1): 69–85.
- Cenedese, G. and Mallucci, E. (2016). What moves international stock and bond markets?, *Journal of International Money and Finance* **60**: 94–113.
- Clark, P. K. (1973). A subordinated stochastic process model with finite variance for speculative prices, *Econometrica* **41**(1): 135–155.
- Davidson, J. (1994). *Stochastic Limit Theory: An Introduction for Econometricians*, Oxford University Press.
- Diebold, F. X. and Yilmaz, K. (2012). Better to give than to receive: Predictive directional measurement of volatility spillovers, *International Journal of Forecasting* **28**(1): 57–66.
- Ehrmann, M., Fratzscher, M. and Rigobon, R. (2011). Stocks, bonds, money markets and exchange rates: measuring international financial transmission, *Journal of Applied Econometrics* **26**(6): 948–974.

- Engle, R. F. and Kroner, K. F. (1995). Multivariate simultaneous generalized ARCH, *Econometric Theory* **11**(1): 122–150.
- Engle, R. F. and Ng, V. K. (1993). Measuring and testing the impact of news on volatility, *The Journal of Finance* **48**(5): 1749–1778.
- Fengler, M. and Herwartz, H. (2018). Measuring spotvariance spillovers when (co)variances are time-varying – the case of multivariate GARCH models, *Oxford Bulletin of Economics and Statistics* **80**(1): 135–159.
- Fisher, L. and Huh, H. S. (2019). Combining sign and parametric restrictions in SVARs by utilising Givens rotations, *Studies in Nonlinear Dynamics and Econometrics* **24**(3): 1–19.
- Francq, C. and Zakoïan, J. (2010). *GARCH Models: Structure, Statistical Inference and Financial Applications*, John Wiley & Sons Ltd.
- Giacomini, R., Kitagawa, T. and Read, M. (2021). Robust Bayesian inference in proxy SVARs, *Journal of Econometrics* .
URL: <https://www.sciencedirect.com/science/article/pii/S0304407621000518>
- Groß-Klußmann, A. and Hautsch, N. (2011). When machines read the news: Using automated text analytics to quantify high frequency news-implied market reactions, *Journal of Empirical Finance* **18**(2): 321 – 340.
- Hafner, C. M. and Herwartz, H. (2008). Analytical quasi maximum likelihood inference in multivariate volatility models, *Metrika: International Journal for Theoretical and Applied Statistics* **67**(2): 219–239.
- Hafner, C. M., Herwartz, H. and Maxand, S. (2020). Identification of structural multivariate GARCH models, *Journal of Econometrics*. (in press).
- Hafner, C. M. and Preminger, A. (2009). On asymptotic theory for multivariate GARCH models, *Journal of Multivariate Analysis* **100**(9): 2044–2054.
- Hemingway, E. G. and O’Reilly, O. M. (2018). Perspectives on Euler angle singularities, Gimbal lock, and the orthogonality of applied forces and applied moments, *Multibody System Dynamics* **44**: 31–56.
- Herrndorf, N. (1984). A functional central limit theorem for weakly dependent sequences of random variables, *Annals of Probability* **12**(1): 141–153.
- Hoffman, D. K., Raffenetti, R. C. and Ruedenberg, K. (1972). Generalization of Euler angles to n -dimensional orthogonal matrices, *Journal of Mathematical Physics* **13**(4): 528–533.
- Horn, R. A. and Johnson, C. R. (2012). *Matrix Analysis, 2nd Ed*, Cambridge University Press.
- Jentsch, C. and Lunsford, K. G. (2019). Asymptotically valid bootstrap inference for proxy SVARs, *Working Papers 190800*, Federal Reserve Bank of Cleveland.
- Kilian, L. and Lütkepohl, H. (2017). *Identification by Sign Restrictions*, Themes in Modern Econometrics, Cambridge University Press, pp. 421–490.
- Kremer, M., Lo Duca, M. and Holló, D. (2012). CISS - a composite indicator of systemic stress in the financial system, *Working Paper Series 1426*, European Central Bank.
URL: <https://ideas.repec.org/p/ecb/ecbwps/20121426.html>

- Lanne, M., Lütkepohl, H. and Maciejowska, K. (2010). Structural vector autoregressions with Markov switching, *Journal of Economic Dynamics and Control* **34**(2): 121–131.
- Lütkepohl, H. and Schlaak, T. (2021). Heteroscedastic proxy vector autoregressions, *Journal of Business & Economic Statistics* pp. 1–14.
- Lunsford, K. G. (2015). Identifying structural VARs with a proxy variable and a test for a weak proxy, *Technical report*, Federal Reserve Bank of Cleveland.
- Mertens, K. and Ravn, M. O. (2013). The dynamic effects of personal and corporate income tax changes in the united states, *American Economic Review* **103**(4): 1212–1247.
- Primiceri, G. (2005). Time varying structural vector autoregressions and monetary policy, *The Review of Economic Studies* **72**(3): 821–852.
- Rigobon, R. (2003). Identification through heteroskedasticity, *Review of Economics and Statistics* **85**(4): 777–792.
- Rigobon, R. and Sack, B. (2003). Measuring the reaction of monetary policy to the stock market, *The Quarterly Journal of Economics* **118**(2): 639–669.
- Romer, C. D. and Romer, D. H. (2010). The macroeconomic effects of tax changes: Estimates based on a new measure of fiscal shocks, *American Economic Review* **100**(3): 763–801.
- Stock, J. H. and Watson, M. (2012). Disentangling the channels of the 2007-09 recession, *Brookings Papers on Economic Activity* **43**(1): 81–156.
- Stock, J. H. and Watson, M. (2016). Dynamic factor models, factor-augmented vector autoregressions, and structural vector autoregressions in macroeconomics, *Handbook of Macroeconomics*, Vol. 2, Elsevier, chapter Chapter 8, pp. 415–525.
- Stock, J. H. and Watson, M. W. (2018). Identification and estimation of dynamic causal effects in macroeconomics using external instruments, *The Economic Journal* **128**(610): 917–948.
- Taylor, J. B. and Uhlig, H. (eds) (2016). *Handbook of Macroeconomics*, Vol. 2, Elsevier.
- Weber, E. (2010). Structural conditional correlation, *Journal of Financial Econometrics* **8**(3): 392–407.

A Narrative corroboration

Structural shocks to the stock market	
Date	Event
04-Aug-1998	U.S. stock markets decline amid growing concerns over Asian economic pressures and political uncertainty around the impeachment of Clinton.
27-Aug-1998	U.S. stock markets decline amid concerns over a global economic downturn due to Russian market turmoil and ruble slide.
31-Aug-1998	U.S. stock markets decline amid uncertainty over the political and economic future of Russia and signs of an economic slow down in the U.S.
19-Apr-1999	U.S. stock markets decline amid investor flight from technology stocks.
23-Sep-1999	U.S. stock markets decline amid weakening dollar and growing concerns that the Fed may raise interest rates at next meeting.
15-Oct-1999	U.S. stock markets decline amid news of rising wholesale inflation and a warning by Greenspan.
04-Jan-2000	U.S. stock markets decline amid Fed rate hike fears.
18-Feb-2000	U.S. stock markets decline amid Fed rate hike fears despite lame inflation news after Greenspan's semi-annual Humphrey-Hawkins testimony; Double witching adds to volatility.
07-Mar-2000	U.S. stock markets decline amid a surprise profit warning from a big blue chip prompting investors to sell-off old economy stocks.
14-Apr-2000	NASDAQ crash and Dot-Com crisis until March 2003; Activation of circuit breakers at the NYSE due to fear sales because of rising inflation and overvalued tech companies.
02-Jan-2001	U.S. stock markets decline amid growing concerns about falling index of manufacturing prompting technology and industry stocks to plunge.
12-Mar-2001	Black Monday; U.S. and global stock market crash following the credit rating downgrade of the U.S. sovereign debt by S&P.
17-Sep-2001	U.S. stock markets decline as trading resumes following 9/11 terrorist attacks; Dow Jones industrial average suffers its worst point-loss in history.
29-Jan-2002	U.S. stock markets decline after Tyco International sparkles worries that more companies will downwardly restate financial results like Enron before going bankrupt. Recent bankruptcies of Enron, Kmart and Global Crossing.
15-Apr-2005	U.S. stock markets decline amid weak New York Empire State index, weak Consumer Sentiment index and IBM's earnings miss.
20-Jan-2006	U.S. stock markets decline amid earnings jitters and rising oil prices due to Iran's nuclear ambitions; Dow and S&P post biggest one day drop in nearly 3 years.
27-Feb-2007	Federal Home Loan Mortgage Corporation (Freddie Mac) announces that it will no longer buy the most risky subprime mortgages and mortgage-related securities.
26-Jul-2007	U.S. stock markets decline amid concerns about credit, housing markets and energy prices; Homebuilding companies D.R. Horton and Pulte Homes post huge losses; Commerce Department reports sharp drop in new home sales in June.
19-Oct-2007	U.S. stock markets decline amid fears about credit and housing sector, earnings, record-high oil prices and the slide in the USD; Wachovia's earnings fall beyond forecasts due to credit market turmoil.
01-Nov-2007	Citigroup downgrade by CIBC analyst reinvigorates credit concerns fueling fears that other major financial players were harder hit by this summer's subprime crisis than originally anticipated.
05-Feb-2008	U.S. stock markets decline amid ISM services index showing business activity falling in January for the first time in five years. Comments by Richmond Fed President Jeffrey Lacker suggest risks of a recession (stagflation).
06-Jun-2008	Crude prices' largest one-day advance ever (oil price shock) and the biggest one-month surge in over 20 years in the unemployment rate.
04-Sep-2008	U.S. stock markets decline amid mixed retail sales reports, weak job market news and an oil price slide magnifying fears about a global slowdown.
15-Sep-2008	Lehman Brothers Holdings Inc. bankruptcy. Bank of America announces its intent to purchase Merrill Lynch & Co.
29-Sep-2008	U.S. House of Representatives rejects the Emergency Economic Stabilization Act of 2008 (bailout plan); Stock market crash.
20-Jan-2009	Financial shares decline among weak earnings and after Royal Bank of Scotland (RBS) warned that it may report a loss of USD 41.3 billion – the biggest loss in British corporate history – on Monday.
01-Oct-2009	U.S. stock markets decline amid Supply Management's September ISM index unexpected fall and weekly jobless claims jumping more than expected.
04-Feb-2010	U.S. stock markets decline amid China curbing lending and sovereign debt issues in Greece, Portugal and Spain.
27-Apr-2010	Global stock markets decline after Greece's sovereign credit rating downgrade by S&P to junk four days after the activation of an EU-IMF bailout; EUR declines. European sovereign debt crisis severs.
06-May-2010	Flash Crash of 2010.
11-Aug-2010	U.S. stock markets decline after Fed announcement of QE2 the previous day; VIX spike.
28-Jan-2011	U.S. and Japan receive sharp warnings from IMF and rating agencies to tackle their budget deficits; Economic indicators below expectations.
22-Feb-2011	Global stock markets decline amid tensions in the Middle East and North Africa (Libya) sending oil and gold prices soaring.
01-Jun-2011	U.S. stock markets decline after Moody's cut Greece's bond rating by three notches to Caa1 in even lower junk level.
02-Aug-2011	U.S. stock markets decline after fiscal cliff and worries about the U.S. economy.
04-Aug-2011	Global stock markets decline due to continuing high foreclosure rates in the U.S. and the European debt crisis (Italy, Spain); Vix spike (uncertainty shock).
08-Aug-2011	Global stock markets decline due to the widening eurozone government debt crisis and Friday's U.S. rating downgrade.
07-Nov-2012	Global stock markets decline amid U.S. fiscal cliff and weak economic outlook for economic growth in Europe; Mario Draghi warns of an economic slowdown in Germany in the course of European debt crisis.
25-Feb-2013	U.S. stock markets decline amid political uncertainty in Italy connected to the European debt crisis. Vix spike (uncertainty shock).
15-Apr-2013	Global stock markets decline amid report of Boston explosions; China reports economic growth slow down in Q1; Gold price plunges.
24-Jan-2014	Global stock markets decline amid emerging market bond and currency turmoil surrounding the fragile five (Brazil, India, Indonesia, SA and Turkey).
31-Jul-2014	Global stock markets decline amid Argentinian debt crisis.
25-Sep-2014	U.S. stock markets decline amid worries about global growth (economic slowdown in Europe, no more stimulus measures in China) and geopolitical tension (Ukraine conflict); VIX spikes.

Table 6: Narrative corroboration of the lower 1%-quantile of the equity shock of the unrestricted BEKK model of the system of daily log returns of the S&P 500 Composite Index (SP500), the yield of the U.S. constant maturity 10 year treasury note (FRTCM10) and the Finex U.S. Dollar Index (NDXC500) from 1/1/1998 to 12/31/2014 when using the stock market index (Z_1) and bond market sentiment (Z_2) TRMIs as proxy variables. News items are extracted from market reports on money.cnn.com and news articles from the Wall Street Journal news archive on wsj.com.

Structural shocks to the bond market

Date	Shock	Event
30-Apr-1998	2.5518	Inflation and unemployment data quell fears of a Fed interest rate hike.
27-Aug-1998	2.4515	U.S. stock markets decline amid Russian ruble crisis causing investors to flock to the relative safety of government securities.
10-Sep-1998	4.0574	Economic and political uncertainty over emerging markets, Russia's economic restructuring and U.S. President Bill Clinton's grip on power.
05-Oct-1998	2.5082	Global economic meltdown over emerging market turmoil (Asia, Russia, Brazil).
03-Feb-2000	2.4631	Fed decision to raise interest rates and expected outlook of interest rate hike. Fed announcement of cut back of issuance of long-term debt causes inversion of the yield curve.
22-Feb-2000	2.6358	Inflation data causes treasury bond rally.
20-Jul-2000	3.0104	Fed Monetary Policy report and economic testimony to Congress by Alan Greenspan; U.S. stock market declines amid profit and rate concerns.
05-Dec-2000	3.7927	Greenspan Speech to America's Community Bankers proffering the possibility of interest cuts next year due to economic cool-down; Resolution of presidential election.
02-Jan-2001	3.2043	U.S. stock markets decline amid growing concerns about falling index of manufacturing activity.
18-Apr-2001	2.5140	Fed surprise announcement to cut short-term interest rates by an aggressive half-percentage point to avert a recession.
08-Aug-2001	3.3438	Fed Beige Book Report and better-than-expected auction of new 10-year notes.
13-Sep-2001	3.8082	First day of official trading after 9/11 pushing treasury yields to historic lows.
26-Jun-2002	2.5152	Fed interest rate announcement. WorldCom Inc. accounting scandal and SEC investigations among big companies causing investors to flock to the relative safety of government securities.
31-Jul-2002	2.7118	Fed Beige Book Report shows worse-than-expected economic reports. U.S. stock markets decline amid profit warnings in the chip and retail sectors.
07-Nov-2002	2.7725	U.S. stock markets decline in a sell-off after a months rally. Previous day's Fed decision to cut interest rates surprisingly sharply signals concerns with weakening U.S. economy.
06-May-2003	2.4345	Fed decision to leave interest rates unchanged; Warning about the risks of continued economic weakness.
05-Mar-2004	3.8268	U.S. payroll and unemployment data showing slowest pace in wage growth in 18 years and persistent unemployment.
15-Jun-2004	3.3906	Greenspan testimony suggesting that inflation was likely to be contained enough to allow for measured rate hike.
06-Aug-2004	2.6565	U.S. payroll and employment data below estimates and concern about oil supply around Yulkes woes causing surge in oil prices.
03-Dec-2004	2.7216	U.S. payroll and employment data below estimates.
04-Feb-2005	2.6553	U.S. payroll and employment data below estimates.
31-Aug-2005	3.6312	Hurricane Katrina raises concerns about the mounting pressures on the U.S. economy from rising energy prices. Prospect of a flat or inverted treasury yield curve.
02-Jun-2006	2.5729	U.S. payroll data below estimates; Data on home prices and manufacturing activity signal economic cool-down.
26-Nov-2007	3.2121	U.S. stock markets slide into correction amid investor concerns that the financial and housing market crisis could send the economy into a recession causing investors to flock to the relative safety of government securities.
15-Sep-2008	3.5972	Lehman Brothers Holdings, Inc. files for Chapter 11 bankruptcy protection and Bank of America announces its intent to purchase Merrill Lynch & Co. for USD 50 billion causing investors to flock to the relative safety of government securities.
04-Nov-2008	2.4869	U.S. presidential election day with Obama as prospective winner. Efforts of U.S. and world governments to stimulate cash flowing to the economy.
25-Nov-2008	3.2765	Fed announcement of QE1
16-Dec-2008	3.8105	Fed decision for aggressive rate cut. Longer-term treasury notes rise amid uncertainty about the bailout of the auto industry. U.S. and European stock markets decline. Prospects of Fed using unconventional tools, e.g. buying longer-dated treasury debt to keep cash flowing to the economy as official lending rates fall toward zero. Regional manufacturing data below estimates and inflation data leading to deflation concerns.
18-Mar-2009	7.3030	Fed's USD 300B pledge to purchase long-term Treasuries over the next six months.
29-May-2009	2.4599	Business activity data in the Midwest below estimates and drop in ISM-Chicago Purchasing Managers Index signals economic cool-down. Upwards correction at U.S. government market after wave of heavy selling Wednesday as mortgage investors shed Treasuries to hedge against rising rates.
10-Sep-2009	2.4555	Fed Beige Book Report raises new concern about consumer spending. Fed statement that rapid rate hike improbable given weakness of global economy.
16-Nov-2009	2.5876	Fed chairman Ben Bernanke speech to the Economic Club of New York stating that economic headwinds will restrain the pace of the U.S. recovery and that reduced bank lending and a weak labour market continue to justify low interest rates.
16-Aug-2010	2.7043	Growing concerns about the global economic outlook (Japan) cause investors to flock to the relative safety of government securities.
13-Sep-2010	2.4036	Fed purchase of USD 3.4 billion in treasury debt as part of the Fed's plan to reinvest cash back into the bond market to help the economic recovery and correction on U.S. government bond markets.
04-Nov-2010	3.8146	Fed announcement of QE2 on 03-Nov-2010 causes yields on U.S. government bonds to fall.
08-Jul-2011	2.6512	U.S. job data for June below estimates.
29-Jul-2011	3.4123	American Debt Crisis and Q2 GDP report below estimates.
09-Aug-2011	6.3727	Fed statement to keep interest rates near historic lows through late 2014. Fed chief Ben Bernanke leaves the door wide open to QE3.
25-Jan-2012	2.5402	Fed statement to keep interest rates below estimates rekindling doubts about strength of recovery. U.S. jobs report well below estimates raises concerns about the pace of the economic growth causing investors to flock to the relative safety of government securities.
06-Apr-2012	2.5742	U.S. payroll and employment data below estimates rekindling doubts about strength of recovery. U.S. jobs report well below estimates raises concerns about the pace of the economic growth causing investors to flock to the relative safety of government securities.
30-May-2012	2.5846	European Debt Crisis (Spanish banking system) causes investors to flock to the relative safety of U.S. government securities.
22-Aug-2012	2.5062	Fed appears ready to take action e.g. by bond buying to stimulate the economy according to FOMC minutes.
18-Sep-2013	3.9394	Fed surprise announcement not to slow down the pace of its bond purchases yet.
14-Oct-2014	3.0677	Global stock market decline amid fears of a global economic slowdown, fighting in the Middle East, geopolitical tensions between West and Russia and the spread of the Ebola virus cause investors to flock to the relative safety of government securities.

Table 7: Narrative corroboration of the upper 1%-quantile of the bond shock of the unrestricted BEKK model of the system of daily log returns of the S&P 500 Composite Index (SP500), the yield of the U.S. constant maturity 10 year treasury note (FRTCM10) and the Finex U.S. Dollar Index (NDXC500) from 1/1/1998 to 12/31/2014 when using the stock market index (Z_1) and bond market sentiment (Z_2) TRMIs as proxy variables. News items are extracted from market reports on money.cnn.com and news articles from the Wall Street Journal news archive on wsj.com.

Structural shocks to the fx market

Date	Shock	Event
23-Jan-1998	3.0030	Asian financial and fx markets crisis, plunge in Asian currencies.
08-Apr-1998	2.5871	The USD loses over one Yen on talk of Japanese tax cut; stock prices slide on more worries about tech sector.
28-Aug-1998	4.4628	Russian tremors on Wall Street. The USD fell against the Japanese Yen after Tokyo stock market slide and against the German mark.
07-Oct-1998	5.4038	Yen's spectacular climb against the dollar continues. USD plunge against the Japanese Yen.
08-Jun-1999	3.2069	Comments from OPEC spur rally in oil futures. Gold falls.
06-Dec-1999	2.8206	White House has no plans to tap oil reserves to offset high prices. Gold falls. The USD weakens against Yen, the EUR slides to parity with the USD. Worries about rising rates evaporate over positive employment data.
03-Jan-2000	3.6997	The USD is lower against the Yen and the EUR.
12-May-2000	3.4002	Crude oil hits USD 30. USD gains on EUR, but slides against Yen. Stocks rally on U.S. gains. ECB interest rate decision.
03-Apr-2001	2.9949	Dollar soars against Yen as Japan outlook worsens. Crude-Oil futures hit lowest level of the year.
17-Sep-2001	5.3010	Trading resumed for the first time after 9/11. Markets are down and gold and oil rally. The dollar finished little changed against the EUR and Yen.
07-Mar-2002	3.3575	Shares tumble on rate jitters amidst Fed Greenspan testimony. USD sinks against the Yen and the EUR.
17-May-2002	2.8494	Tech stocks gain and Gold prices on the rise.
20-Jun-2002	2.5645	Jump in Oil prices sends trade gap to record level.
08-Jul-2002	2.6248	USD drops against Yen and EUR. Gold stocks continue to soar. Technology stocks dropped.
05-Jun-2003	3.0461	USD plummets against EUR on ECB cut. Weak U.S. job data.
22-Sep-2003	2.9737	Techs drop amid USD weakness. G-7 endorsement of flexible exchange rates lifts Asian currencies.
18-Nov-2003	2.8640	Strong Euro.
30-Sep-2004	2.7684	Dollar weakens against Yen. Tech stocks inch higher, oil price rally.
05-Nov-2004	2.7029	Gold vaults higher on weak USD, oil prices drive ECB to consider a rate increase. China may be ready to loosen Yuan peg.
22-Feb-2005	3.2807	Techs drop amid rising oil prices.
01-Sep-2005	3.0657	U.S. releases oil from reserve to ease crunch in the aftermath of hurricane Katrina. USD falls on oil impact.
06-Oct-2005	3.5692	Stocks fall despite oil slide. Tech shares fall ahead of earnings season.
25-Oct-2005	2.7736	Cold front causing energy prices to jump and stocks to slide. USD slips after Bernanke news.
28-Nov-2005	2.5890	Gold price on the rise. Gold tops USD 500 in after-hours trade.
30-Mar-2006	2.7642	USD declines on Yen and EUR. U.S. officials urge China on markets, Yuan.
30-May-2006	3.2148	Major markets sink amid rising oil prices and sliding U.S. consumer confidence. Paulson appointed Treasury secretary.
24-Nov-2006	2.5682	Stocks fall on weaker USD. Rally in commodities markets.
03-Aug-2007	2.5689	Markets down among credit market fears and Bear Stearns debt rating downgrade. USD falls against the EUR and the Yen.
20-Sep-2007	4.8135	USD dips at an all-time low against the EUR, oil boils, metals shine.
07-Nov-2007	3.2403	Weakening USD, Gold trading higher, Crude oil nears USD100 a barrel.
24-Jan-2008	2.9601	Nasdaq advances on Tech earnings. USD falls versus the Yen and EUR. Gold rallies.
12-Sep-2008	3.0098	Dollar weak, commodity prices down, VIX soaring. Lehman Slides 42%. Euro Rallies on Weak U.S. Data. Fixed-Rate 30-Year Mortgages fall below 6% on bailout news.
17-Sep-2008	3.3380	USD dropped Wednesday against the EUR and against the Yen, after news that the Fed would bail out AIG.
22-Sep-2008	3.3505	Oil: Biggest one-day gain ever. USD gets biggest hit in seven years from treasury plan. Commodities gain across the board as the dollar tumbles.
29-Oct-2008	2.7490	Credit crunch hits trade. USD and EUR rise sharply on Yen. Stocks succumb to bleak Fed outlook. Weakening USD propels dollar-traded commodities.
19-Mar-2009	2.8385	Dollar dips due to Fed statement to buy long-term Treasuries. Fed's announcement dampened the dollar's safe-haven appeal, knocking it down from a three-year peak hit against a basket of currencies earlier in the month.
21-Oct-2009	2.7399	The prospect of U.S. interest rates staying at exceptionally low levels for longer than most other major countries sent the greenback sliding. In turn crude oil and other commodities continued their march higher. VIX falls.
20-May-2010	3.3361	The US dollar rose against a basket of major currencies, while oil fell below USD 69 a barrel. Spot gold prices rose.
01-Jul-2010	3.0012	Gold prices plunge over 3%. EUR recovery: short euro/long gold trade appears to be unwinding.
08-Aug-2011	2.7772	Gold soars to record after U.S. downgrade.
29-Jun-2012	2.7401	EU moves boost EUR. Crude Prices Jump 9.4% buoyed by EU summit and renewed anxiety on Iran. Silver Soars 5.1%. Gold Up 3.5%. Risk currencies also got a boost and the USD weakened. Yuan had its biggest quarterly drop ever.
10-Jan-2013	3.0327	Oil rises on Saudi cutback, explosion in Yemen that halted most of the country's oil exports and bullish Chinese trade data. Signs that the ECB will not cut interest rates any time soon boosted bullion buying.
15-Aug-2013	2.9833	EUR shoots to 18-month high vs. Yen and hit a one-week peak against the USD. Gold prices settle 2% higher on Mideast tensions and violence in Egypt, home to the strategically important Suez Canal and the Sumed pipeline. USD falls in volatile trade after mixed signals from economic data.

Table 8: Narrative corroboration of the upper 1%-quantile of the currency shock of the unrestricted BEKK model of the system of daily log returns of the S&P 500 Composite Index (SP500), the yield of the U.S. constant maturity 10 year treasury note (FRTCM10) and the Finex U.S. Dollar Index (NDXCS00) from 1/1/1998 to 12/31/2014 when using the stock market index (Z_1) and bond market sentiment (Z_2) TRMIs as proxy variables. News items are extracted from market reports on money.cnn.com and news articles from the Wall Street Journal news archive on wsj.com.